Anonymous Referee #1 Received and published: 7 September 2017

The authors are grateful to the referee for the constructive comments and additional grammar corrections. They have been helpful to improve the manuscript significantly. Our responses are addressed point to point hereafter.

This manuscript presents analysis of the spectral properties of shortwave radiation backscattered from melt ponds found on Arctic sea ice during summer. The information presented is well organized, easily readable, and clear. The subject should be of interest to readers. I have only a few minor comments, mostly technical in nature.

p. 2 line 33 photo in Fig 1 shows various evolutionary stages of ponds? not sure there is 'evolution' shown in this image. Rather, this seems to me to be a fair representation of the variety of melt pond colors often seen in a particular view, however, I see no reason to infer this field represents time-dependent changes.
Reply: Indeed, the "evolutionary" is not very accurate. We revised this sentence to "The photograph in Fig. 1 reveals the large variety in melt-pond appearances even on the same ice floe."

p. 5 line 7 "two-dimensional representation works"– would be helpful to add a bit more information here– does the 2D representation completely describe the light field? Better to say that than 'works'.
Reply: Corrected accordingly. We revised this sentence to "These coordinates are dependent, z = 1 - x - y, and as illustrated in Fig. 2b this two-dimensional presentation can determine the given color (Hunt, 2004)".

p.10 line 12 "optically isotropic" is not the same as "isotropic scattering" line 14 same question line 16 pond water 'clear with regard to its optical properties'? not at long wavelengths!
Reply: We revised the terms in lines 12 and 14 into "isotropic scattering". It is exactly what we want to express there. The sentence in line 16 was revised to "it is assumed here that melt pond water is clean and scattering can be neglected (LU16)".

p. 10 line 25 subjects'
Reply: Corrected accordingly. The sentence was revised to "These functions have been determined through a series of experiments that aimed to judge colors while looking through a hole with a 2° field of view".

p. 14 line 2 superliner? not sure 'superliner' means
Reply: The description was not correct in the original manuscript. It should be "nonlinear".

p. 14 line 7 -9 I expect the reason that agreement is better for thin ice is not necessarily associated with ice topography and horizontal homogeneity assumptions of the model, but rather that thinner ice has less optical thickness. With dark ocean beneath, the thinner domain shows better discrimination as light at some wavelengths simply doesn't get backscattered,

and that wavelength cutoff varies quickly with optical thickness.

Reply: We agree with reviewer. We added such interpretation in the revised manuscript at P13 “Another possible explanation comes from ice thickness since thin ice passes through more light than thick ice. With dark ocean beneath, the thinner domain shows a better discrimination as light at some wavelengths simply does not get backscattered, and that wavelength cutoff varies quickly with ice thickness” as explaining the figure.

At P15 “The latter is partly because that the plane-parallel assumption agrees more closely with ponds on flat sea ice than on rough ice, and also possibly due to the higher transparency of thin ice than thick ice” in the conclusion.

Fig 2 relatively little information content here

Reply: The original Figure 2 (Schematic graph of the radiative transfer model) was removed accordingly. The model was explained by text in P3.

Fig 4 why does pure bubble-free ice have higher absorption than sea ice? Sea water really has higher absorption than ice? These relative values surprise me, so I think they merit some comment in the text.

Reply: The absorption coefficients employed in the study came from different references. Data of the absorption coefficient of water came from Smith and Baker (1981). Data of the absorption coefficient of pure ice came from Grenfell and Perovich (1981) (> 400 nm) and Warren (1984) (< 400 nm). According to these data, the absorption coefficient of water is a little higher than that of pure ice in the 560-780 nm band, but lower than that of pure ice in the 380-560 nm band.

The absorption coefficient of sea ice is a weighted-average of that of water and pure ice according to Perovich (1996), its values are closer to pure ice than to seawater because of the large volume fraction of pure ice. Sometimes, the absorption coefficient of sea ice is also lower than that of pure ice and seawater, especially as wavelength greater than 560 nm in the figure. This happens only if there are lots of gas bubbles and little brine pockets contained in sea ice, and the absorption by gas bubbles can be ignored but their volume fraction cannot be neglected.

We added the new references into the figure capital as “Figure 3: Absorption coefficients of clean seawater, pure bubble-free ice and sea ice in the visible band. The water data are from Smith and Baker (1981). The pure ice data are from Grenfell and Perovich (1981) and Warren (1984). The $k_{\lambda,i}$ value was calculated from $k_{\lambda,i} = \nu_{pi}k_{\lambda,pi} + \nu_{bp}k_{\lambda,w}$, based on the volume fractions $\nu_{pi} \geqslant 60\%$ and $\nu_{bp} \leqslant 20\%$ ($\nu_{pi} + \nu_{bp} \leqslant 100\%$) from field observations of summer Arctic sea ice (Huang et al., 2013)”.

And we also added comments in P6 as “Note that $k_{\lambda,w}$ is lower than $k_{\lambda,pi}$ for $\lambda < 560$ nm, and higher than $k_{\lambda,pi}$ as $\lambda > 560$ nm. The weighted average $k_{\lambda,i}$ varies closer to $k_{\lambda,pi}$ than to $k_{\lambda,w}$ because of the large volume fraction of pure ice, but sometimes it is also lower than both $k_{\lambda,pi}$ and $k_{\lambda,w}$ especially for $\lambda > 560$ nm (Fig. 3). This happens only if there are lots of gas bubbles and little brine pockets contained in sea ice, and the absorption by gas bubbles is limited but their volume fraction cannot be neglected”.

References

Grenfell, T.C., and D.K. Perovich. 1981. Radiation absorption coefficients of polycrystalline ice from 400–1400 nm. Journal of Geophysical Research, 86: 7447–7450.

Hunt R.G.W. 2004. The reproduction of colour, 6th ed. John Wiley & Sons, pp. 844.

Perovich, D. K. 1996. The optical properties of sea-ice. Cold Reg. Res. and Eng. Lab. (CRREL) Report 96-1, 585 Hanover, NH.

Smith, R.C., and K.S. Baker. 1981. Optical properties of the clearest natural waters (200–800 nm). Applied Optics, 20: 177–184.

Warren, S.G. 1984. Optical constants of ice from the ultraviolet to the microwave. Applied Optics, 23, 1206-1225.

Anonymous Referee #2 Received and published: 23 November 2017

We thank the referee for the comments on our manuscript. The comments have been helpful to improve the manuscript a lot. Our responses are addressed point by point below.

The paper of "the color of melt ponds on Arctic sea ice" give a new insight on the optical properties of Arctic melt pond, which is very important for the knowledge of melt pond thermodynamic processes and remote sensing. There are very few papers have been published on this topic because of the complexity of influencing factors. Thus, it is worthy of publication. However, in the current state, I think this study just can give the knowledge on the color of idealized and simple melt pond because it just give the model of two-layer pond (ice covered by water) and just in the state of overcast sky: (1) Most melt ponds in Arctic would be covered by a thin ice although in the midsummer because the cold air at night, and the snow accumulated on the thin ice and itself would influence the optical characteristics of melt pond, as shown in the Fig.1 (Not all of them are open melt pond) ; (2) overcast sky is prevailing but not always during summer in Arctic and the incident spectrum would obvious influence the pond color. Thus, if the authors can add some works on (1) three- or four- layers model and (2) the influences of incident spectrum, this study would be effectively improved both for the preciseness and applicability.

Reply: (1) We investigated the case that a thin-ice layer is placed on top of the melt pond (three-layer model) in section 3.5 as comparing simulated color with field observations, as some observed melt ponds by Istomina et al. (2016) were indeed covered by a very thin ice layer as the reviewer said. However, the differences in the results determined by an open pond model and an ice-covered pond model are very limited, and less that 3% in the HSL values of the pond color (as shown on Figure A below). That means the influence from the transparent ice layer (1–3 cm) on pond reflection can be ignored.

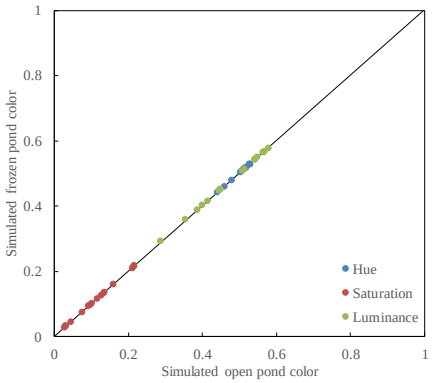

Figure A. Comparison between the simulated color of an open pond and a frozen pond. Note that this figure is only used to show here, and will not be included into the revised manuscript because the comparison in the figure is straightforward and can be explained clearly by text.

(2) The incident solar spectrum is different day to day although under overcast sky conditions. In section 3.2, we selected six different measurements of F_0 according to Grenfell and Perovich (2008), and then investigated the influence of solar spectrum on the color of melt pond. A diffuse incident solar radiation is the basic assumption of the present two-

stream radiative transfer model, so the influence of the direction of solar beam in clear days cannot be investigated in this study. It is the same with the studies in Perovich (1990), Taylor and Feltham (2004), Flocco et al. (2015) who employed the similar two-stream radiative transfer model. Additionally, as the reviewer said, overcast sky is prevailing but not always during summer in Arctic. It is acceptable if most, not all, situations can be treated in a single paper. Of course, we agreed that "further work is still needed to cover clear sky conditions." (in section 4.2 and conclusions).

Here are some other detail comments:

(1) Color can be equivalent to albedo. Color only covers the visible light.

Reply: We agree. Both color and albedo are representations on the spectral radiation reflected back from the pond surface. The differences between them are (1) color covers only the visible band, but albedo covers a larger band, for example, 350 – 950 nm, if measured by a RAMSES radiometer; (2) color can be sensed by CCD cameras or human eyes, but albedo can only be measured by a radiometer. Color is more easily to be measured and observed directly by human eyes, so a study on the color of melt pond is necessary although extensive studies have been conducted on the albedo of melt pond.

(2) Scattering in meltwater and ocean water is neglected. Why?

Reply: We ignored the scattering in water because (1) this has been shown to be a valid approximation for melt ponds with a depth less than 1 m (Podgorny and Grenfell, 1996a; Taylor and Feltham, 2004). (2) The scattering coefficient of pure water is 2-3 orders of magnitude lower than that of sea ice (Smith and Baker, 1981), scattering in water is therefore not a main factor affecting the optics of melt pond as comparing with ice scattering. (3) There are no observations of any optically active impurities in melt ponds to the authors' knowledge. (4) Clear melt ponds are the focus of this study, and dirty ponds with a sediment-covered floor or with cryoconite holes as observed by Eicken et al. (1994) have been excluded. (5) The ocean beneath ice is always regarded as a semi-infinite medium and there is no radiation scattered upward within the ocean, for examples, in Taylor and Feltham (2004), and Lu et al. (2016). As a result, no scattering is an acceptable approximation for meltwater and ocean.

We added these explanations in section 4.1.

(3) 3.3 Influence of optical properties of ice. – how about the porosity of the ice under the melt water. Many cases, the density of ice under melt pond is only about 1/3 of that of level ice because the large porosity and the salinity is as large as the upper ocean.

Reply: Ice porosity is indeed an important parameter of melting sea ice. However, it cannot be directly included into the radiative transfer model in this study. Instead, the influence of ice porosity was investigated through considering ice absorption and scattering coefficients. In Fig. 7a, different values of ice scattering coefficient corresponded to different content of gas bubbles in sea ice, which has been studied in Perovich (1990). In Fig. 7b, the absorption coefficient of sea ice was calculated by the weighted-average of that of water and pure ice, and the ice absorption coefficient is actually determined by the volume fractions of pure ice and brine pockets in sea ice. As a result, although ice porosity is not explicitly included in section 3.3, it poses an impact on both absorption and scattering in sea ice, and further on

the color of melt pond.

We clearly stated these now in section 3.3 as "However, the microstructure and physical properties of sea ice cannot be treated directly by our RTM. In this section, the scattering coefficient σ_i and the absorption coefficient $k_{\lambda,i}$, actually functions of the ice microstructure (Light et al., 2004), are investigated for their impact on pond color".

Also we presented a possibility to fully consider ice porosity in the conclusion section: "In a real melt process, phase transition exists not only at ice surface but also in ice interior. If H_i and H_p are calculated by a thermodynamic model (e.g. Tsamados et a., 2015), and IOPs of sea ice are associated with ice physical parameters (e.g. Light et al., 2004), for example, ice porosity, then the seasonal evolutions in the color and albedo of melt ponds can be determined straightforwardly. However, it is out of the scope of the present paper and can be investigated in further studies".

(4) 4.2 Possibility of retrieving pond depth and ice thickness.—I would like remove this section because: (1) the visible color of pond is very difficult to obtained by satellite remote sensing due to the cloud and small scale of the pond, (2) we cannot judge which pond is covered by ice and/or snow by satellite/aerial images, (3) the color of pond also depends on many factors, especially for the porosity of ice under the ice, it also can be found that the relationship is very unreliable as shown in fig.11.

Reply: We disagree with reviewer on this comment and would still prefer to keep our discussion in this section because:

(1) We were not promoting retrieve ice thickness from melt pond colors that are detected by the satellite data. Instead, we would argue that "hand-held photography, ship-borne photography, and airborne photography are very effective ways to get the small-scale information on ice surface" and to be used to retrieve thin ice thickness. Especially, with the wide applications of unmanned aerial vehicles (UAVs) in sea ice investigations, it is easy for UAVs equipped with a digital camera to get the information of pond color.

(2) It is indeed difficult to judge if the pond is covered by ice or snow by images. However, according to our newly added analyses in section 3.5 and Figure A above, a thin ice cover on top of a melt pond does not change the color of the melt pond very much. So the error introduced by the thin ice cover can be ignore as retrieving ice thickness from pond color. The ponds that covered by snow or thick ice are most likely beyond the Arctic summer season and are therefore excluded from this study.

We have added a new paragraph in section 4.2 to clarify the limitations and applicability of the color-retrieval method, including the text presented in (1) and (2).

(3) The color of melt pond indeed depends on many factors, as we have investigated in sections 3.1, 3.2, and 3.3. However, once we identified the primary factors, the pond color can be determined. And We have improved the retrieve model (c.f. Eq. 7) and the results showed some improvement for thin ice thickness detection:

$$\Delta = |(H,S,L)_{\mathrm{SIM}} - (H,S,L)_{\mathrm{MEA}}| = \sqrt{c_H \cdot (H_{\mathrm{SIM}} - H_{\mathrm{MEA}})^2 + c_s \cdot (S_{\mathrm{SIM}} - S_{\mathrm{MEA}})^2 + c_L \cdot (L_{\mathrm{SIM}} - L_{\mathrm{MEA}})^2}\ , \qquad (7)$$

The parameters c_H, c_S, and c_L indicate the different sensitivity of hue, saturation, and

luminance values of pond color on pond depth and ice thickness, and they are determined by normalizing the square of correlation coefficient R^2 between the HSL values and the measured Hi and Hp. According to the statistical analyses in Istomina et al. (2016), there is c_H = 0.255, c_S = 0.712, and c_L = 0.033 (the Table to calculate these values was included in the revised manuscript).

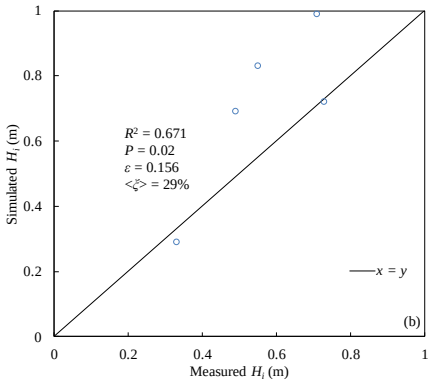

Figure B. This is a subset of ice-thickness retrievals for H_i < 1 m. R is the correlation coefficient between simulated and measured H_i. P is the significance level of the correlation. ε is the root-mean-square error, and <ξ> is the mean of relative error in simulated H_i.

The different sensitivity of hue, saturation, and luminance values of pond color on H_i and H_p were considered using the parameters c_H, c_S, and c_L in Eq. (7). Then the results of ice thickness retrievals were improved. Especially for thin ice H_i < 1 m (Figure B), the correlation coefficient between simulated and measured ice thickness R^2 = 0.671 and the correlation is significant (P = 0.02). The relative error ξ between simulated and measured values presents an average of 29%.

We think the result is acceptable considering available data is very limited. More validations from field observations in future are needed in order to improve the retrieve model and reduce the errors.

References

Eicken, H., Alexandrov, V., Gradinger, R., Ilyin, G., Ivanov, B., Luchetta, A., Martin, T., Olsson, K., Reimnitz, E., Pac, R., Poniz, P. and Weissenberger, J. 1994. Distribution, structure and hydrography of surface melt puddles, Ber. Polarforsch, 149, 73–76.

Flocco, D., D.L. Feltham, E. Bailey, and D. Schroeder. 2015. The refreezing of melt ponds on Arctic sea ice, J. Geophys. Res. Oceans, 120, 647–659, doi:10.1002/2014JC010140.

Grenfell, T.C., and D.K. Perovich. 2008. Incident spectral irradiance in the Arctic Basin during the summer and fall, J. Geophys. Res., 113, D12117, doi:10.1029/2007JD009418.

Istomina, L., Melsheimer, C., Huntemann, M., Nicolaus, M. and Heygster, G. 2016. Retrieval of sea ice thickness during melt season from in situ, airborne and satellite imagery, IEEE International Geoscience and Remote Sensing Symposium (IGARSS), Beijing, 7678–7681, doi: 10.1109/IGARSS.2016.7731002.

Light, B., Maykut, G. A. and Grenfell, T.C. 2004. A temperature-dependent, structural-optical

model of first-year sea ice, J. Geophys. Res., 109, C06013, doi:10.1029/2003JC002164.

Lu, P., M. Leppäranta, B. Cheng, and Z. Li. 2016. Influence of melt-pond depth and ice thickness on Arctic sea-ice albedo and light transmittance, Cold Reg. Sci. Technol., 124, 1–10, doi:10.1016/j.coldregions.2015.12.010.

Perovich, D.K. 1990. Theoretical estimates of light reflection and transmission by spatially complex and temporally varying sea ice covers, J. Geophys. Res., 95(C6), 9557–9567.

Podgorny, I.A., and T.C. Grenfell. 1996a. Partitioning of solar energy in melt ponds from measurements of pond albedo and depth, J. Geophys. Res., 101(C10), 22737–22748.

Podgorny, I.A., and T.C. Grenfell. 1996b. Absorption of solar energy in a cryoconite hole, Geophys. Res. Lett., 23, 2465–2468.

Skyllingstad, E.D., and C.A. Paulson. 2007. A numerical study of melt ponds, J. Geophys. Res., 112, C08015, doi:10.1029/2006JC003729.

Skyllingstad, E.D., C.A. Paulson, and D.K. Perovich. 2009. Simulation of melt pond evolution on level ice, J. Geophys. Res., 114, C12019, doi:10.1029/2009JC005363.

Smith, R.C., and K.S. Baker. 1981. Optical properties of the clearest natural waters (200–800 nm). Applied Optics, 20: 177–184.

Taylor, P.D., and D.L. Feltham. 2004. A model of melt pond evolution on sea ice, J. Geophys. Res., 109, C12007, doi:10.1029/2004JC002361.

Tsamados, M., Feltham, D., Petty, A., Schroeder, D. and Flocco, D. 2015. Processes controlling surface, bottom and lateral melt of Arctic sea ice in a state of the art sea ice model, Phil. Trans. R. Soc. A, 373, 20140167, doi:/10.1098/rsta.2014.0167.

Anonymous Referee #3 Received and published: 29 November 2017

The authors are grateful to the referee for the constructive comments that helped to improve the manuscript substantially. Our responses to the comments are addressed point by point below.

General Comment: This paper describes investigation of the color of melt pond on the Arctic sea ice simulated by the radiative transfer model and validation using field observations. Such sensing and analyzing melt pond may become increasingly important for detecting progress of warming in the Arctic Ocean. Therefore, I recommend this paper for publication. However, I have a couple of major and minor comments that should be considered.

Major comment 1): In section 3.1, the authors mention the effects of melt depth and underlying ice thickness (P6. L18 – P7. L5). In addition, the effects of albedo and color of melt pond are also considered. The authors describe the pond color depends on underlying ice thickness and the possibility of estimation of ice thickness from the pond color. Basically, the pond color on first-year ice (FYI) containing brine and sea water indicates various gray depending on pond depth. The pond color on multi-year ice (MYI) displays green and blue. Thus the pond color also depends on underlying ice types (FYI or MYI). I recommend to add a description about the effect of ice type difference for same ice thickness. This explanation is expected to make the validity of this manuscript increase.

Reply: We added new descriptions on the effect of ice type on pond color in section 3.1 as "Basically, melt ponds on FYI in Arctic are shallow and flat, resulting in various gray color tones, while MYI melt ponds are always deep and narrow, displaying green and blue (Polashenski et al., 2012; Webster et al., 2015). These agree well with the variations in Fig. 4f".

Major comment 2): I agree the result of the comparisons with field observations described in section 3.5. However, the description of the quantitative measurements for pond color by Istomina et al. (2016) is incomplete. Fog appears frequently during summer and observation of pond color seem to be affected by fog. The authors should mention the influence of fog during summer.

Reply: We agree with reviewer. The fog will give impact on the pond color, especially if one took the photos from a distance, e.g. from helicopter or something like that. In Istomina et al. (2016), "fog indeed happened during the field work, but the hand-held camera was very close to the measured ponds and the work was stopped for heavy fog conditions", so the influence of fog on the obtained pond color was limited in this study.

We have added a detailed description on how the pond color was photographed during field investigations in the revised manuscript.

Major comment 3): According to Fig. 11, a good agreement can be found for thin ice with ice thickness < 1 m (P12. L19-L20). I would like to suggest that the color-retrieval method using a RTM is useful to estimate thin ice thickness because sea ice thickness has been declined in recent years. This is not discussed in a convincing way. In order to understand the argumentations given in the manuscript, I recommend to add discussion about when and

where the color-retrieval method is useful. I think the valid area and period of the color-retrieval method are mainly ice edge and in late-summer, respectively.

Reply: Thank you for this very good comment. A new paragraph was now added to the end of section 4.2 to tell the limitations and applicability of the color-retrieval method. It mainly includes:

(1) This method is valid for thin ice with thickness less than 1 m, and when the melt ponds on top of ice are open or just covered by very thin ice. Frozen melt ponds with a snow or thick ice cover, having an obviously different appearance from open ponds, are excluded from this method.

(2) Overcast sky conditions are preferable for this method. They are prevailing although not always present during summer in Arctic.

(3) It is still difficult for the satellite instruments to detect melt-pond color because of the small spatial scale of melt ponds. In contrast, hand-held photography, ship-borne photography, and airborne photography are very effective ways to get the small-scale information on ice surface and provide a basis for ice thickness retrievals. Especially, with unmanned aerial vehicles (UAVs) equipped with a digital camera it is easy to observe sea ice surface features, including melt-pond color, at a floe scale.

Major comment 4): The manuscript describes that the result shown in Fig. 11 is still encouraging (P13. L1-L5). However, it is difficult to agree a new way of determining the sea-ice thickness. To clarity the validity of the color-retrieval method using RMT, I recommend to redraw plots of the ice thickness less than 1 m and more than 1 m separately in Fig. 11b. Adding the correlation coefficients, significance levels, and root mean square errors in Fig. 11 is also recommended.

Reply: Revised accordingly. We have improved the retrieve model and the results showed some improvement for thin ice thickness detection. A subplot for $H_i < 1$ m was also presented and all necessary statistical parameters were included.

Please check our reply to the last comment of Referee #2 for details.

Minor comments:

1) P2-L1: Studies on melt ponds area more than three aspects. For example, the studies using synthetic aperture radar and passive microwave sensor should be included. There are not many papers about remote sensing of melt pond by satellite. Recently Tanaka et al. (2016) reported estimation of melt pond fraction using satellite microwave radiometer. I recommend to cite their paper in this section. Tanaka, Y., K. Tateyama, T. Kameda, and J. K. Hutchings (2016), Estimation of melt pond fraction over high concentration Arctic sea ice using AMSR-E passive microwave data, J. Geophys. Res. Oceans, 121, doi:10.1002/2016JC011876.

Reply: Thanks for your recommendation. Satellite remote sensing on melt pond has been included in the three aspects we stated on P2. And we now added the new reference there.

2) P3-L14: RTM was investigated the dependence of apparent optical properties (AOPs), particularly albedo and transmittance, on sky conditions, pond depth, ice thickness, and the inherent optical properties (IOPs) of ice and water (Lu et al., 2016). That is worth mentioning as well. For example, it would be essential to show about the broadband albedo were higher

on overcast days than on clear days by 0.01 in August.

Reply: The AOPs of melt ponds have been investigated thoroughly in Lu et al. (2016), and therefore were not the subjective of the present study. The color of melt pond is the focus here rather than the surface albedo.

References

Istomina, L., Melsheimer, C., Huntemann, M., Nicolaus, M. and Heygster, G. 2016. Retrieval of sea ice thickness during melt season from in situ, airborne and satellite imagery, IEEE International Geoscience and Remote Sensing Symposium (IGARSS), Beijing, 7678–7681, doi: 10.1109/IGARSS.2016.7731002.

Polashenski, C., Perovich, D. and Courville, Z.: The mechanisms of sea ice melt pond formation and evolution, J. Geophys. Res., 117, C01001, doi:10.1029/2011JC007231, 2012.

Webster, M. A., Rigor, I. G., Perovich, D. K., Richter-Menge, J. A., Polashenski, C. M. and Light, B.: Seasonal evolution of melt ponds on Arctic sea ice, J. Geophys. Res. Oceans, 120, doi:10.1002/2015JC011030, 2015.

J. Hutchings (Editor) Received and published: 27 November 2017

The authors are grateful to the editor for the constructive comments. These comments have been helpful to improve the manuscript a lot. Our responses to the comments are addressed point by point.

Dear Peng Lu and co-authors, Thank you for your contribution. I am interested in receiving your response to the reviews. I have provided some additional comments below. At this stage I have not checked the paper for continuity. I do note that the paper is well written and English clear (thank you), and as I expect you will make some substantial revisions to the paper I am holding off on a through proof-read until after revision.

Please consider another paper in the Cryosphere Discussion that is on the topic of reflectance of melt ponds. I would be very interested in your opinion on the complimentary nature of your work to this. You can find the paper at https://www.the-cryospherediscuss.net/tc-2017-150/tc-2017-150.pdf, or I can send you a pdf if you need.
Reply: Thanks for your promotion. Actually Larysa Istomina and Georg Heygster in that paper Malinka et al. (2017), are also co-authors of this paper.

In Malinka et al. (2017), a RTM for melt ponds different to ours is developed based on Makshtas and Podgorny (1996), and the melt-pond reflectance was estimate by using their RTM, and pond depth and ice thickness were also retrieved using measured spectral albedo. The latter part of Malinka et al. (2017) has the same focus with the discussions in section 4.2 of our paper, but the models and the parameters employed to retrieve are different with each other. We also now cited their results in the conclusion part as "A recent publication by Malinka et al. (2017) suggested another way to determine pond depth and ice thickness from measured spectral albedo of melt ponds. They obtained better retrievals of Hi and Hp partly because they used more complicated spectra as input compared with our case.".

We think these two papers not only prove that problems on melt ponds are really focus of scientists, but also can promote the improvements in the scientific field through academic debate.

In general, please check that you are citing the original source of information. Was Polashenski and Perovich (2012), line 15, page 2, the original source of the 7 stage model for albedo evolution in summer? I recall Hajo Eicken and Don Perovich talking about this much earlier.
Reply: We checked the paper of Perovich and Polashenski (2012). The seven-phase evolution is a main finding of that paper, and was also clearly stated in the abstract section of Perovich and Polashenski (2012). So it should be the original source.

I am curious, could your model be extended to clear skies with non-diffuse illumination? Would this allow you to identify the thickness of ice under melt ponds from satellite imagery such as provided by MODIS? Is this inverse problem one you considered? How much influence does assuming overcast skies have on the comparison with in-situ observations? Did you only consider the sub-set of overcast data in the comparison, or does this include data for all skies?

Reply: (1) A diffuse incident solar radiation is the basic assumption of the present radiative transfer model, so non-diffuse illumination under clear skies cannot be investigated in this study. It is the same with the studies of Perovich (1990), Taylor and Feltham (2004), Flocco et al. (2015) who employed the similar two-stream radiative transfer model for sea ice or melt pond. Besides, overcast sky is prevailing although not always during summer in Arctic. It is acceptable if most situations can be treated in this paper.

(2) The spatial scale of melt ponds is small as comparing with the resolution of satellite instruments such as MODIS. So we think it is very difficult to observe pond color by satellite remote sensing, as one of the reviewers said. But hand-held photography, shipboard photography, and aerial photography are very effective ways to get the small-scale information on ice surface. Especially, with the wide applications of unmanned aerial vehicles (UAV) in sea ice investigations, it is easy for UAVs equipped with a digital camera to get the information of pond color although within a relative small scale. During Chinese Arctic Expeditions, such kind of equipment has been tested and pictures were obtained. This is exactly what we considered the inverse problem for.

We now added a new paragraph in section 4.2 to clearly state the limitations and applicability of the color-retrieval method, including the ideas presented in (1) and (2).

(3) During in-situ observations, the sky conditions were reported overcast during the optical measurements. It agreed with the assumption in the present model, and the influence of the assumption on the comparison can be ignored. We now add a detailed description on field conditions during the measurements of Istomina et al. (2016).

In the figure captions, I assume "true color" refers to the modeled color of the melt pond. Can you clarify.

Reply: Yes, it is the “simulated color”.

I had some difficulty in following your discussion on retrieval of ice thickness from pond color. I feel you need to clarify the discussion as to the parameters that confound the inverse solution. It would help to provide the evidence for this. In particular, the paragraph on lines 10-15, page 12, is vague what the competing parameters in the sky and ice conditions are and how they counteract each other such that it might not be possible to find a single solution based on melt pond color. Given you are justifying the value of your work based on the possibility of developing ice thickness products from satellite and camera observations I feel this needs to be addressed much more carefully in your analysis and discussion.

Reply: We revised the section 4.2 and the revised contents include:

(1) Pond color is a function of pond depth, underlying ice thickness, IOPs of sea ice, and incident solar radiation in the present study. Among them, pond depth and underlying ice thickness are the primary factors according to the sensitivity analyses, and IOPs and incident solar radiation can be assigned with empirical constants for melting sea ice in summer. Then there is (color) = $f(H_i, H_p)$, and the inverse problem we focused on is $(H_i, H_p) = f^{-1}$(color).

(2) The paragraph on lines 10-15, page 12 is a little confusing because it provided a comparison between Fig. 10 (results of the positive problem) and Fig. 11 (results of the inverse problem). So we removed this paragraph, and focused only on the inverse problem in section 4.2.

(3) The retrieving model to solve the inverse problem was now improved in Eq. (7), and different contributions from the hue, saturation, and luminance values of pond color were considered according to the statistical analyses in Istominia et al. (2016). Then the retrievals of ice thickness were highly improved as comparing with in-situ measurements, especially for thin ice with $H_i < 1$ m. It also argued for the possibility of our method.

Details can be seen in our reply to the last comment of Referee #2.

(4) We added a new paragraph in section 4.2 to clarify the limitations and applicability of the color-retrieval method. Satellite remote sensing is not the direct application of the method. Instead, UAVs equipped with a digital camera are able to get the information of pond color within a relative small scale, and such equipment has also been tested during Chinese Arctic Expeditions. More validations are of course necessary to improve the robustness of the method, but at least in present, the possibility of the new method is still encouraging.

Please consider acknowledging those who collected the data you use in this study. Looking forward to your response, Jenny

Reply: Yes, we added such acknowledgement: "The authors are grateful to the scientific party of the ARK 27/3 cruise for making the sea ice optical measurements possible. Special thanks are expressed to Marcel Nicolaus for organizing the logistics and to the Sea Ice Physics group on board for assisting with the measurements. Three anonymous reviewers and the editor Jennifer Hutchings are also acknowledged for their constructive comments to highly improve the manuscript".

References:

Flocco, D., D.L. Feltham, E. Bailey, and D. Schroeder. 2015. The refreezing of melt ponds on Arctic sea ice, J. Geophys. Res. Oceans, 120, 647–659, doi:10.1002/2014JC010140.

Istomina, L., Melsheimer, C., Huntemann, M., Nicolaus, M. and Heygster, G. 2016. Retrieval of sea ice thickness during melt season from in situ, airborne and satellite imagery, IEEE International Geoscience and Remote Sensing Symposium (IGARSS), Beijing, 7678–7681, doi: 10.1109/IGARSS.2016.7731002.

Makshtas, A. P. and Podgorny, I. A. 1996. Calculation of melt pond albedos on arctic sea ice, Polar Res., 15 (1), 43-52.

Malinka, A., Zege, E., Istomina, L., Heygster, G., Spreen, G., Perovich, D., and Polashenski, C. 2017. Reflective properties of melt ponds on sea ice, The Cryosphere Discuss., https://doi.org/10.5194/tc-2017-150, in review.

Perovich, D. K. and Polashenski, C. 2012. Albedo evolution of seasonal Arctic sea ice, Geophys. Res. Lett., 39, L08501, doi:10.1029/2012GL051432.

Perovich, D.K. 1990. Theoretical estimates of light reflection and transmission by spatially complex and temporally varying sea ice covers, J. Geophys. Res., 95(C6), 9557–9567.

Taylor, P.D., and D.L. Feltham. 2004. A model of melt pond evolution on sea ice, J. Geophys. Res., 109, C12007, doi:10.1029/2004JC002361.

The color of melt ponds on Arctic sea ice

Peng Lu[1], Matti Leppäranta[2], Bin Cheng[3], Zhijun Li[1], Larysa Istomina[4], Georg Heygster[4]

[1]State Key Laboratory of Coastal and Offshore Engineering, Dalian University of Technology, Dalian, 116024, China
[2]~~Department of Physics~~[2]Institute of Atmospheric and Earth Sciences, University of Helsinki, Helsinki, Fi-00014, Finland
[3]Finnish Meteorological Institute, Helsinki, Fi-00101, Finland
[4]Institute of Environmental Physics, University of Bremen, Bremen, 28359, Germany

Correspondence to: Peng Lu (lupeng@dlut.edu.cn)

Abstract. Pond color, which creates the visual appearance of melt ponds on Arctic sea ice in summer, is quantitatively investigated ~~in this study. A~~using a two-stream radiative transfer model ~~is used~~ for ponded sea ice~~: the~~. The upwelling irradiance from the pond surface is determined, and then ~~the upwelling~~its spectrum is transformed into the RGB color space through a colorimetric method. The dependence of pond color on various factors such as water and ice properties and incident solar radiation is investigated. The results reveal that increasing underlying ice thickness H_i enhances both the green and blue components of pond color, whereas the red component is mostly sensitive to H_i for thin ice (H_i < 1.5 m) and to pond depth H_p for thick ice (H_i > 1.5 m), similar to the behavior of melt-pond albedo. The distribution of the incident solar spectrum F_0 with wavelength affects the pond color rather than its ~~level~~intensity. The pond color changes from dark blue to brighter blue with increasing scattering in ice, ~~but~~and the influence of absorption in ice on pond color is limited. The pond color reproduced by the model agrees well with field observations on Arctic sea ice in summer, which supports the validity of this study. More importantly, the pond color has been confirmed to contain information about meltwater and underlying ice, and therefore it can be used as an index to retrieve H_i and H_p. ~~The results show that retrievals~~Retrievals of H_i for thin ice (H_i < 1 m) agree better with field measurements than retrievals for thick ice, but ~~that retrievals~~those of H_p are not good. ~~Color has been shown to be~~The analysis of pond color is a new potential method to obtain ice thickness information~~, especially for melting sea ice~~ in summer, although more validation data and improvements to the radiative transfer model will be needed in future.

1 Introduction

Melt ponds are the most distinctive characteristic of Arctic sea ice surface during summer. They can cover up to 50% of the ice surface (Webster et al., 2015) and lower the surface albedo from as high as 0.8 (snow) to as low as 0.15 (Perovich and Polashenski, 2012). The albedo evolution generates a positive ice-albedo feedback mechanism, which enhances the melting of ice, alters the physical and optical properties of sea ice, and even affects the salt and heat budget of the ocean surface layer (Landy et al., 2015). As a result, melt ponds are an issue as important and inevitable as the dramatic decay of current Arctic sea ice (Flocco et al., 2012).

Studies on melt ponds can be categorized with respect to three aspects: morphological observations, optical measurements, and modeling of the melting processes. Morphological studies focus on the distribution and physical properties of melt ponds using field observations and remote sensing (e.g. Huang et al., 2016). The melt-pond distribution determined by aerial photography was linked to the areally averaged surface albedo (Perovich et al., 2002b), and an obvious decrease in average surface albedo was discovered by comparing image-derived data with historical observations (Lu et al., 2010). A distinct variation trend in melt-pond fractions (MPF) in different regions of the Arctic Ocean has been found (Istomina et al, 2015) using ~~melt pond fraction~~MPF retrievals from satellite optical data (Rösel et al., 2012; Zege et al., 2015). Satellite passive microwave data were also employed to estimate MPF over high-concentration Arctic sea ice (Tanaka et al., 2016), serving as a basis for building time series of MPF in regions of consolidated ice pack. In-situ measurements of ice physics were carried out to demonstrate the mechanisms that enable melt-pond formation (Polashenski et al., 2012), and a newly found percolation blockage process was identified to be responsible for initial meltwater retention on highly porous first-year ice (FYI) (Polashenski et al., 2017).

Optical measurements focus mainly on the partition of solar radiation in melting sea ice (e.g. Nicolaus and Katlein, 2013). The melt-pond albedo has been found to vary with the melt stage of Arctic sea ice, and the seasonal evolution of ice albedo can be ~~described by a~~categorized into seven ~~phase classification~~ phases: cold snow, melting snow, pond formation, pond drainage, pond evolution, open water, and freezeup (Perovich and Polashenski, 2012). The transmittance through FYI was almost three times larger than through multiyear ice (MYI) according to measurements made using a remotely operated vehicle under summer sea ice. It resulted from the larger melt-pond coverage of FYI compared to MYI (Nicolaus et al., 2012). Ice thickness, scattering in ice, and melt-pond distribution were found to be primary factors dominating light transmission through ponded sea ice, although their impacts were different on small and large scales (Light et al., 2015; Katlein et al., 2015).

Finally, numerical simulations have been used to investigate the physical processes of melt ponds from formation to summertime development and then to autumn refreezing (e.g., Tsamados et al., 2015). A three-dimensional model was used to simulate the evolution of melt ponds and found that the role of snow ~~was~~is important mainly at the onset of melting, whereas initial ice topography strongly ~~controlled~~controls pond size and fraction throughout the melt season (Scott and Feltham, 2010). The refreezing process of melt ponds was also modeled, and the results revealed that ice growth would be overestimated by 26% if the impact of trapped ponds was excluded (Flocco et al., 2015). New parameterizations for melt ponds have also been embedded into climate models to evaluate the role of surface melting on the summer decay of Arctic sea ice (e.g. Holland et al., 2012). The improved models produced results that agreed more closely with observations than other models without or only implicitly including the effect of melt ponds (Flocco et al., 2012; Hunke et al., 2013).

This study focuses on the color evolution of melt ponds on Arctic sea ice, a perspective on melt ponds that has seen ~~very~~ few investigations so far (Perovich et al., 2002a; Light et al., 2015; Istomina et al., 2016). The photograph in Fig. 1 reveals ~~various~~

~~evolutionary stages of~~the large variety in melt ~~ponds.~~ pond appearances even on the same ice floe. The color of melt ponds ~~can be~~varies from light bluish ~~or~~to dark, largely depending on the age of the pond and the properties of the underlying ice, which can be easily examined during field investigations. First quantitative measurements on melt-pond color have been performed in the Central Arctic in 2012 (Istomina et al., 2016). Except for spectral albedo of sea ice and melt ponds measured with the portable radiometer ASD FieldSpecPro 3 (Istomina et al., 2013; Istomina et al., 2017), a photograph has been taken at each albedo measurement site, together with ice thickness and water depth measured by means of drilling. These field data show a clear connection between the underlying ice thickness of the melt pond and its color and spectral albedo. The effect of the water depth was found to be negligible. It has been suggested that the melt pond color can therefore be used for ice thickness estimates in summer (Istomina et al., 2016).

The motivation of this study is to elaborate on this idea and understand why the color of melt ponds can change and the micro-physical and optical reasons leading to such changes. Efforts will also be made to find ways to use the information provided by pond color more effectively because this color contains the optical response of melt ponds and sea ice to incident solar radiation. For example, information ~~can be obtained from color~~ about sea-ice thickness below the melt pond, pond depth, and primary production in melt ponds could be retrieved.

To achieve these objectives, a radiative transfer model (RTM) initially developed to parameterize melt-pond albedo (Lu et al., 2016, hereafter LU16) ~~was~~is used. Section 2 introduces the color-retrieval method using the RTM. Section 3 investigates the influences of various factors, including pond depth, ice thickness, incident solar radiation, and inherent optical properties (IOPs), on melt-pond color. Section 4 discusses model uncertainty and retrievals from pond color, and Section 5 draws conclusions.

2 Methods

2.1 Radiative transfer model for melt pond

~~The~~Albedo sensed by spectral radiometers represents the spectrum upwelling irradiance from the surface, but the color of a melt pond is actually the response of human eyes ~~or imaging sensors to the radiation upwelling from the pond surface~~to this irradiance, which consists of the reflected solar radiation ~~reflected by~~from the pond surface and the backscattering radiation from ice and water below. Based on the spectral RTM for melt ponds in LU16, each part of the upwelling radiation can be determined, thus providing the necessary information to determine pond color.

For the ~~three~~two-layer model ~~shown in Fig. 2~~comprising of melt pond and underlying ice, radiation transfer ~~was~~is simplified as two streams, upwelling and downwelling irradiances. These are governed by two coupled first-order differential equations under the assumptions of diffuse incident solar radiation and isotropic scattering (Flocco et al., 2015). Assuming continuity of

radiation fluxes at ~~each interface in Fig. 2~~air-pond, pond-ice, and ice-ocean interfaces, the irradiance in both directions in each layer can be calculated as well as the melt-pond albedo α_i (see Eqs. (1–9) in LU16 for ~~detailed information~~details).

2.2 Estimation of pond color from spectrum

Along the whole solar spectrum, only the portion in the visible band, the wavelengths between λ_1 = 380 nm and λ_2 = 780 nm, is detectable by human eyes. To derive the color of an outgoing spectrum from the pond surface, $F_a(\lambda) = \alpha_i F_0(\lambda$~~,~~) where $F_0(\lambda)$ is the incident solar irradiance, the two following methods are proposed.

The first is a mathematical method defining the color as the mean wavelength of the spectral distribution of light:

$$\bar{\lambda} = \frac{\int_{\lambda_2}^{\lambda_1} \lambda F_a(\lambda) d\lambda}{\int_{\lambda_2}^{\lambda_1} F_a(\lambda) d\lambda}, \quad (1)$$

where $\bar{\lambda}$ represents the 'mean color' of the melt pond. For example, $\bar{\lambda}$ = 475 nm denotes a blue color, 510 nm green, and 570 nm yellow.

The second approach is ~~the~~a colorimetric method ~~provided by the International Commission on Illumination (CIE). It is~~ based on the fact that human eyes with normal vision have three kinds of cone cells, which sense light with spectral sensitivity peaks at ~~short (420–440~~long (560–580 nm), middle (530–540 nm), and ~~long (560–580~~short (420–440 nm) wavelengths. International Commission on Illumination (CIE, 1986) defines three color matching functions, $\bar{x}(\lambda)$, $\bar{y}(\lambda)$, and $\bar{z}(\lambda)$, as numerical description of the chromatic response of ~~an~~a standard observer to an incident spectrum (Fig. ~~3a~~2a). Note that the peaks of color matching functions in Fig. 2a shift a little from those of cone cells above, and it is because modifications are necessary to avoid the mathematical difficulty as representing the color by negatives (Hunt, 2004). The tristimulus values in the XYZ color space for a reflective surface are given by:

$$\begin{cases} X = \frac{1}{N}\int_{\lambda_2}^{\lambda_1} \alpha_\lambda \cdot F_0(\lambda) \cdot \bar{x}(\lambda) d\lambda \\ Y = \frac{1}{N}\int_{\lambda_2}^{\lambda_1} \alpha_\lambda \cdot F_0(\lambda) \cdot \bar{y}(\lambda) d\lambda \\ Z = \frac{1}{N}\int_{\lambda_2}^{\lambda_1} \alpha_\lambda \cdot F_0(\lambda) \cdot \bar{z}(\lambda) d\lambda \\ N = \int_{\lambda_2}^{\lambda_1} F_0(\lambda) \cdot \bar{y}(\lambda) d\lambda \end{cases}, \quad (2)$$

where Y is a measure of the perceived luminosity of the light and the X- and Z- components give the chromaticity of the spectrum. N is defined as the reference illuminant for the reflective surface, and the luminosity value (Y) is constrained in the range of 0–1.

The CIE XYZ color space can describe all colors visible to humans, but is not convenient for use in computer graphics or by a common output device such as an LED monitor. Therefore, the values in the XYZ space ~~must be~~are converted into an RGB space, which specifies intensity values for red, green, and blue primary light to generate a desired color. This can be done by a linear transformation as:

$$\begin{bmatrix} X \\ Y \\ Z \end{bmatrix} = M \begin{bmatrix} r \\ g \\ b \end{bmatrix} = \begin{bmatrix} X_r & X_g & X_b \\ Y_r & Y_g & Y_b \\ Z_r & Z_g & Z_b \end{bmatrix} \begin{bmatrix} r \\ g \\ b \end{bmatrix} = M^{-1} \begin{bmatrix} X \\ Y \\ Z \end{bmatrix} = \begin{bmatrix} X_r & X_g & X_b \\ Y_r & Y_g & Y_b \\ Z_r & Z_g & Z_b \end{bmatrix}^{-1} \begin{bmatrix} X \\ Y \\ Z \end{bmatrix}, \tag{3}$$

where r, g, and b are the intensities of red, green, and blue primaries that yield the desired color and M is the transformation matrix consisting of the coordinates of the three primaries in the XYZ space.

To obtain the matrix M, the CIE chromaticity diagram must be introduced (Fig. ~~3b~~2b), which describes a color in a two-dimensional chromaticity coordinate system (x, y) while ignoring its luminance Y. The XYZ coordinates are thus scaled as:

$$\begin{cases} x = X/(X+Y+Z) \\ y = Y/(X+Y+Z) \\ z = Z/(X+Y+Z) \end{cases}. \tag{4}$$

These coordinates are dependent, $z = 1 - x - y$, and ~~therefore a~~as illustrated in Fig. 2b this two-dimensional presentation ~~works (Fig. 3b~~can determine the given color (Hunt, 2004). For a given RGB space, the chromaticity coordinates are always given as the primary colors (x_r, y_r), (x_g, y_g), (x_b, y_b) and the white point (x_w, y_w).

According to Eq. (4), the transformation matrix M can be expanded as:

$$M = \begin{bmatrix} X_r & X_g & X_b \\ Y_r & Y_g & Y_b \\ Z_r & Z_g & Z_b \end{bmatrix} = \begin{bmatrix} (X_r+Y_r+Z_r)x_r & (X_g+Y_g+Z_g)x_g & (X_b+Y_b+Z_b)x_b \\ (X_r+Y_r+Z_r)y_r & (X_g+Y_g+Z_g)y_g & (X_b+Y_b+Z_b)y_b \\ (X_r+Y_r+Z_r)z_r & (X_g+Y_g+Z_g)z_g & (X_b+Y_b+Z_b)z_b \end{bmatrix}$$

$$= \begin{bmatrix} x_r & x_g & x_b \\ y_r & y_g & y_b \\ z_r & z_g & z_b \end{bmatrix} \begin{bmatrix} X_r+Y_r+Z_r & 0 & 0 \\ 0 & X_g+Y_g+Z_g & 0 \\ 0 & 0 & X_b+Y_b+Z_b \end{bmatrix} = A \cdot S, \tag{5}$$

where the matrix A is known from Fig. ~~3b~~2b. To obtain the unknown diagonal matrix S, the definition of the white point is used. The rgb intensities for the white point are $r = g = b = 1$. The luminosity is not specified in Fig. ~~3b~~2b; a full luminance can be used for the white point according to Eq. (2), that is, $Y_w = 1$. Substituting these values into Eq. (3):

$$\begin{bmatrix} X_w \\ Y_w \\ Z_w \end{bmatrix} = \begin{bmatrix} X_r & X_g & X_b \\ Y_r & Y_g & Y_b \\ Z_r & Z_g & Z_b \end{bmatrix} \begin{bmatrix} 1 \\ 1 \\ 1 \end{bmatrix} = M \begin{bmatrix} 1 \\ 1 \\ 1 \end{bmatrix} \Rightarrow [X_w + Y_w + Z_w] \begin{bmatrix} x_w \\ y_w \\ z_w \end{bmatrix} = A \cdot S \cdot \begin{bmatrix} 1 \\ 1 \\ 1 \end{bmatrix}$$

$$\Rightarrow \frac{Y_w}{y_w} \begin{bmatrix} x_w \\ y_w \\ z_w \end{bmatrix} = A \cdot \begin{bmatrix} X_r + Y_r + Z_r \\ X_g + Y_g + Z_g \\ X_b + Y_b + Z_b \end{bmatrix} \Rightarrow \begin{bmatrix} X_r + Y_r + Z_r \\ X_g + Y_g + Z_g \\ X_b + Y_b + Z_b \end{bmatrix} = A^{-1} \cdot \begin{bmatrix} x_w / y_w \\ 1 \\ z_w / y_w \end{bmatrix}. \quad (6)$$

By combining Eqs. (5) and (6), the transformation matrix M is determined, and then the *rgb* intensities can be calculated using the XYZ coordinates according to Eq. (3).

Comparing the two methods, the first one is straightforward, and the result is a mean wavelength corresponding to a monochromatic light, which is not particularly good to compare with human vision or to present by computer graphics according to Fig. ~~3b~~2b. The second method is complex, but gives the intensity of the three primaries, so that it provides a convenient way to reproduce color on a computer. The following analyses mainly focus on the results of the latter method.

3 Results

To calculate radiative transfer and color retrieval, certain parameters must to be specified. The IOPs of sea ice and water have been fully discussed in LU16, and ~~therefore their~~the results are used here. The absorption coefficients of sea ice and water ($k_{\lambda,i}$, $k_{\lambda,w}$) are shown in Fig. ~~4~~3. The former is a weighted average of contributions from pure ice and brine pockets, $k_{\lambda,i} = v_{pi}k_{\lambda,pi} + v_{bp}k_{\lambda,w}$ (Perovich, 1996) and varies within ±20% due to varying combinations of the volume fractions of pure ice v_{pi} and brine pockets v_{bp} (Huang et al., 2013). The mean curve of $k_{\lambda,i}$ in Fig. ~~4 is defined as the absorption coefficient of Arctic sea ice in summer.~~3 is defined as the absorption coefficient of Arctic sea ice in summer. Note that $k_{\lambda,w}$ is lower than $k_{\lambda,pi}$ for $\lambda < 560$ nm, and higher than $k_{\lambda,pi}$ as $\lambda > 560$ nm. The weighted average $k_{\lambda,i}$ varies closer to $k_{\lambda,pi}$ than to $k_{\lambda,w}$ because of the large volume fraction of pure ice, but sometimes it is also lower than both $k_{\lambda,pi}$ and $k_{\lambda,w}$ especially for $\lambda > 560$ nm (Fig. 3). This happens only if there are lots of gas bubbles and little brine pockets contained in sea ice, and the absorption by gas bubbles is limited but their volume fraction cannot be neglected. Scattering in meltwater and ocean water is neglected ($\sigma_{\lambda,w} = 0$). The scattering coefficient of sea ice is independent of wavelength because the scattering inhomogeneities in ice are much larger than the wavelength of light. A value of $\sigma_i = 2.5$ m $^{-1}$ has been promoted by LU16 for summer Arctic sea ice. The incident solar irradiance $F_0(\lambda)$ measured by Grenfell and Perovich (2008) under a completely overcast sky on August 7, 2005 with the solar disk not visible is used because it is representative of the Arctic summer, as in LU16. The chromaticity coordinates (x, y) of the primaries are (0.640, 0.330), (0.210, 0.710), and (0.150, 0.060) for red, green, and blue respectively and (0.313, 0.329) for the white point in the selected Adobe RGB color space (Adobe, 2005). These parameters are constant throughout the study unless otherwise defined.

3.1 Influence of pond depth and ice thickness

According to experience and field observations, pond depth H_p and underlying ice thickness H_i are the two main factors influencing melt-pond albedo as well as color (Light et al., 2015; Istomina et al., 2016). Here, H_p ~~was~~is assumed to vary between 0 and 0.5 m and H_i between 0.5 and 5.0 m. The range of ice thickness is somewhat beyond the current state in the Arctic summer (Lang et al., 2017). However, it is still beneficial to see the outcome of the proposed model at limiting conditions of thick deformed MYI. The results are shown in Fig. ~~5~~4.

It is clear that the apparent optical properties of the melt pond are totally different for thin and thick ice. In Fig. ~~5a~~4a, the melt-pond albedo is sensitive to H_i for thin ice, but to H_p for thick ice, as also illustrated by LU16. The mean wavelength of pond color as retrieved by Eq. (~~3~~1) has similar features (Fig. ~~5b~~4b). However, the behavior of the three primary colors is somewhat different. The red component in Fig. ~~5c~~4c increases mostly with increasing H_i for thin ice (H_i < 1.5 m), but with increasing H_p for thick ice (H_i > 1.5 m), similarly to the wavelength-integrated albedo α_B in Fig. ~~5a. However, the~~ 4a. The green and blue components in Figs. ~~5d~~4d and ~~5e~~4e change only with H_i and almost not at all with H_p, except for very thick ice with H_i > 4 m. As a result, the ~~true~~simulated color of the melt pond made up of the RGB components, as shown in Fig. ~~5f~~4f, gradually changes from dark blue to bright blue with increasing underlying ice thickness. However, for thin ice of H_i < 1.5 m, the slight influence of H_p on pond color is also detectable. In other words, deeper pond water makes the color bluish rather than gray because red light is more easily absorbed by pond water. ~~The simulated pond color can be~~Basically, melt ponds on FYI in Arctic are shallow and flat, resulting in various gray color tones, while MYI melt ponds are always deep and narrow, displaying green and blue (Polashenski et al., 2012; Webster et al., 2015). These agree well with the variations in Fig. 4f. The simulated pond color can be also compared with photographs during field investigations on Arctic sea ice in summer, such as in Fig. 1, which shows results that are visually close to Fig. ~~5f~~4f. Furthermore, the part with thinner underlying ice seems obviously darker than the rest (Fig. 1), agreeing with the trend revealed by Fig. ~~5f~~4f. More quantitative validations of pond color using field observations are presented in Section 3.5.

3.2 Influence of incident solar radiation level

Sky conditions of course affect the appearance of the ocean surface, but they are not considered here because of the assumption of diffuse incident radiation in the model ~~(Fig. 2). Only~~. In this case, only the level of incident solar radiation, $F_0(\lambda)$, can be altered to investigate the influence on pond color. Except for the default value of $F_0(\lambda)$ on August 7 defined previously, five more irradiance spectra were selected according to Grenfell and Perovich (2008). All of them represent Arctic summer conditions under a completely overcast sky in August and September 2005 (Fig. ~~6a~~5a). In their work, the Arctic sky was never totally clear near the solar noon in August, but in September, cloud cover decreased somewhat, providing cloud-free periods. There is also a difference in the noon solar zenith angle between August and September at 70 °N–80 °N: it is 60 °–70 °in August and 70 °–80 °in September. These six cases differ widely with respect to $F_0(\lambda)$. Like LU16, H_p = 0.3 m and H_i = 1.0 m are used,

corresponding to a clear water pond on typical Arctic FYI, and they are constant in following discussions unless otherwise defined. The results are shown in Fig. ~~6b~~5b.

It is surprising that the influence of $F_0(\lambda)$ on pond color is less pronounced than that of H_i and H_p in Fig. ~~5~~4. The *rgb* intensities of pond color changed little under an overcast sky in August, so was the ~~true~~simulated color shown on the top of Fig. ~~6b~~5b. However, the results on overcast days in September, which produce a weaker red light but stronger blue light, ~~were different, resulting in a much~~show a brighter color than in August. $F_0(\lambda)$ was the only variable that could have caused the change. However, according to Fig. ~~6a~~5a, the incident spectra differed widely from each other and therefore were not the direct reason for the similar results in Fig. ~~6b~~5b.

If a normalized value of the incident irradiance is defined as $\omega = F_0(\lambda) / \int_{\lambda_2}^{\lambda_1} F_0(\lambda) d\lambda$, the difference is obvious according to Fig. ~~7~~6. The level of F_0 on an overcast day decrease with date in Fig. ~~6a~~5a, and ω varies with obviously stronger energy in the shortwave band (< 530 nm), but less energy in the longwave band (> 530 nm). This trend becomes more pronounced with time according to Fig. ~~7~~6. As a result, the color of the melt pond in September includes more contributions from blue light, but fewer from red light (Fig. ~~6b~~5b).

3.3 Influence of optical properties of ice

Optically active inclusions in sea ice, gas bubbles, brine pockets, and biota affect the appearance and color of melt ponds on summer Arctic sea ice (Kilias et al., 2014). However, the microstructure and physical properties of sea ice cannot be treated directly by our RTM. In this section, the scattering coefficient σ_i and the absorption coefficient $k_{\lambda,i}$, actually functions of the ice microstructure (Light et al., 2004), are investigated for their impact on pond color. The results are shown in Fig. ~~8~~7.

The scattering coefficient of sea ice ranges from 1.2 to 2.5 m $^{-1}$ ~~in Fig. 8a~~, corresponding to sea ice from melting blue ice with a small content of gas bubbles to porous white ice containing large quantities of gas bubbles according to Perovich (1990). The ~~extreme case of~~full range starting from $\sigma_i = 0$ is ~~also~~ presented (Fig. 7a) to understand the model outcome for an idealized purely absorbing medium. Without scattering, the melt-pond albedo is ~~$\alpha_p =$~~ 0.05, reflecting only specular reflectance at the air-water interface, and the *rgb* intensities of pond color are all at ~~very~~ low level, producing a dark grey color. With σ_i increasing into a realistic range, both the albedo and the *rgb* intensities increase obviously, making the pond color brighter.

For $k_{\lambda,i}$, the absorption coefficient of sea ice in Fig. ~~8b~~7b, the maximum and minimum values are determined from different combinations of volume fractions of pure ice and brine pockets (Fig. 4). With enhanced absorption in sea ice, the role of scattering in ice becomes less important, weakening the resulting upwelling irradiance, and the albedo and the *rgb* intensities consequently decrease. However, their changes are small compared with those shown in Fig. ~~8a~~7a, and the resulting variation in pond color is nearly undetectable.

The comparison in Fig. ~~8~~7 clearly illustrates the importance of scattering in ice, which is the source of upwelling irradiance from the pond water and the ice interior ~~(Fig. 2).~~. When scattering in ice is enhanced, the upwelling red, green and blue light from the pond surface will all be enhanced, with the red component enhanced less, producing a light blue pond color.

3.4 Variations during ice melt

It is interesting to see how the pond color develops during the process of ice melting. However, a complex thermodynamic model of sea ice would be needed to model in detail the changes in ice thickness and pond depth. For simplicity, an idealized model was used under the assumption of mass conservation, $H_i + \delta H_p = 1.3$ m, where δ is the ratio of water density ρ_w to ice density ρ_i, equal to 1.3 for porous ice in summer (Huang et al., 2013). Drainage of meltwater into the ocean and basal melt of sea ice were not considered to emphasize the influence of surface melting on pond color.

During sea-ice melting, as shown in Fig. ~~9~~8, the ice thickness decreases from 1.3 m to 0, and the melt pond deepens from 0 to 1 m. At the same time, the pond albedo drops from 0.5 to 0.05, and the *rgb* intensities of pond color also decrease from about 0.6 to 0.05, resulting in an evolution of the pond color from gray to blue and then to almost black.

It is also noteworthy that variations in the red band are different from those in the green and blue bands. First, the red intensity is lower overall than that of the other bands during the melting process, which can be attributed to the fact that ice and water absorb red light more thoroughly than green and blue light (Fig. ~~4~~3). Second, the red intensity ~~seems to drop~~drops nearly linearly along with ice melt, but the green and blue intensities drop ~~obviously~~ faster at the end of ice melting than at the beginning. Red decreases linearly here because it is absorbed by the growing pond, whereas green and blue can maintain higher scattering because they can penetrate the pond almost to the end.

3.5 Comparisons with field observations

Validation of results is important, especially for the new method presented here, but most in-situ observations of pond color are visual and qualitative. The only quantitative measurements found for pond color were conducted by Istomina et al. (2016) on the Arctic sea-ice surface during the R/V Polarstern cruise ARK27/3 IceArc 2012. ~~A~~In addition to a portable spectroradiometer used for albedo measurements, a digital camera was used to take photographs of melt ponds, and the color information in the HSL (hue-saturation-luminance) color space was extracted to associate with concurrently measured pond

depth and underlying ice thickness. The sky conditions were overcast during the optical measurements. Fog occurred frequently but its effect was limited, because the hand-held camera was close to the measured ponds and the work was stopped for heavy fog conditions. Additionally, some melt ponds observed by Istomina et al. (2016) were covered with a newly formed ice layer (1–3 cm). A new ice layer was then added to the RTM in section 2.1 to treat this situation, but the differences between an open pond and a refrozen pond were determined to be less than 3% in the primaries of the pond color. The influence of the transparent ice layer on pond reflection is therefore ignored.

Using the measured values for H_i and H_p, the pond color can be reproduced and compare with the in-situ observations~~, as shown on~~ (Fig. ~~10.~~9). Note that the *rgb* intensities calculated by the present model have been transformed into HSL values (0–1) to match the data in HSL color space reported by Istomina et al. (2016).

The simulated pond color ~~in HSL color space~~ agrees well with the in-situ measurements by Istomina et al. (2016). The measured H_p was in the range of 8–40 cm and H_i in the range of 33–256 cm, producing varying pond color with a hue value in the 0.2–0.5 range, a saturation value within 0–0.5, and a luminance value within 0.4–0.6. The correspondingly simulated hue, saturation, and luminance values of pond color were within 0.4–0.5, 0–0.3, and 0.3–0.6 respectively. The agreement is acceptable because H_i and H_p are the only variables in the present model, but in-situ environmental conditions such as sky conditions and ice optics were different from pond to pond and of course not completely consistent with the definitions in the model. In other words, this experiment underlines the importance of H_i and H_p in determining the surface appearance of melt ponds (LU16) compared with other impact factors discussed above.

Obvious divergence can be found only at individual points. For examples, points a and b in Fig. ~~10~~9 belong to the same melt pond with H_i = 0.33 m and H_p = 0.2 m, but the proposed model produced a relatively large difference in the hue and luminance values of pond color compared with other points. This pond is special because it has the thinnest underlying ice layer among all the measurements. It is suspected to be a mature melt pond that will melt through to the underlying ocean, in which case the brine channels in the underlying ice layer should be much larger and denser than in other cases, with different IOPs from the present model. Point c belongs to another melt pond that has the largest saturation value among all measurements of pond color, but the proposed model reproduced a lower value.

4 Discussions

4.1 Uncertainties in pond-color estimation

Color is a highly subjective parameter associated with human visual perception, and therefore different people will have different descriptions even of the exact same color. Although colorimetry has provided tools to quantify and describe physically

human color perception, it is still difficult to reproduce accurately the color of a reflecting surface (Fig. ~~10~~9). This is true especially in the Arctic Ocean, with its severe weather conditions. Therefore, it is important to understand the limitations and uncertainties of the present method.

The first question arises from the assumption of the RTM in Section 2.1, in which diffuse incident radiation is assumed and scattering must be taken as isotropic. The former assumption is not a major problem in the summer Arctic due to the frequent presence of low stratus cloud cover. The latter assumption may, however, be inappropriate for sea ice, which possibly has more forward scattering than backward scattering, but actually most studies have still treated scattering in sea ice as ~~optically~~ isotropic (Katlein et al., 2014). Moreover, internal melting makes sea ice more porous in summer, and as a result the geometric structure of ice becomes more irregular, which can favor isotropic scattering (e.g., Leppäranta et al., 2003). Consequently, one may expect that the ~~isotropic~~ assumption of isotropic scattering is not ~~badly~~much biased for melting sea ice. Besides, it is assumed here that melt pond water is ~~clear with regard to its optical properties~~clean and scattering can be neglected (LU16). This is ~~a good approximation~~ true if the water is ~~true~~ meltwater from snow, ~~but~~and is also acceptable for ice meltwater or percolated Arctic sea water. ~~In fact, there~~There are no observations of any optically active impurities in melt ponds to the authors' knowledge~~.~~, and the approximation has been shown valid for melt ponds shallower than 1 m (Podgorny and Grenfell, 1996). Dirty ponds with a sediment-covered floor or with cryoconite holes as observed by Eicken et al. (1994) are not considered here, and frozen melt ponds with a ~~thin~~snow or thick ice cover in autumn (Flocco et al., 2015) are also excluded from this study~~, although either sediments or ice cover would cause variations in pond color. This study focuses only on clean melt ponds without ice cover during the melt season~~.

The second question arises from the definition of the colorimetric method as retrieving the RGB components from a spectrum. Three color matching functions $\bar{x}(\lambda)$, $\bar{y}(\lambda)$, and $\bar{z}(\lambda)$, are used in Eq. (2) to quantify the chromatic response of the observer. These functions have been determined through a series of experiments that ~~had the subjects'~~aimed to judge colors while looking through a hole ~~that allowed them~~with a 2 ° field of view (Wright, 1928; Guild, 1931). By 1960s, new color matching functions corresponding to a 10 ° standard observer were developed (Stiles and Birch, 1959). The 10 ° observer is currently believed to provide the best representation of the average spectral response of human observers, although the 2 ° observer still has its place for measuring objects that will be viewed at a distance. In addition, various RGB color spaces such as sRGB, Apple RGB, and Adobe RGB have been defined to satisfy the display of colors on different kinds of output devices (Süsstrunk et al., 1999), and they have different chromaticity coordinates for red, green, blue, and white colors in Fig. 3b. Tests have revealed that the differences between the two functions and among various RGB color spaces are not large enough to produce significantly different pond colors in this study, and therefore these results are not presented here.

The third question is associated with field observations of the color of melt ponds. Digital cameras used during field observations always have a ~~different~~ viewing angle different from the standard observer defined previously, thus producing a

different response to the incident spectrum. Besides, the color on photographs highly depends on the camera and the photographic parameters such as ISO and aperture values (Istomina et al., 2016), also making the direct comparisons of pond color between simulated results and field measurements difficult. Istomina et al. (2016) used RAW photographic data, which can save much more information about the light field during field observations than common image formats such as JPG, to calculate pond color. In addition, the incident solar radiation reaching the ice surface changes continuously in the Arctic Ocean, but for simplification, a constant F_0 was used in this study as a representative condition of the Arctic summer. However, the results shown in Fig. ~~6~~5 illustrate that the influence of F_0 is not as important as the contributions from other impact factors.

4.2 Possibility of retrieving pond depth and ice thickness

Like melt-pond albedo, pond color is also affected by many factors. Among them, pond depth and underlying ice thickness are the most important according to earlier discussions. Pond color can therefore be expressed by a function such as ~~(color)~~$C = f(H_i, H_p)$~~.)~~ if other impact factors discussed in Section 3 are treated as empirical constants. This implies a possibility of using pond color to retrieve H_i and H_p ~~if~~through solving the inverse problem~~ can be solved~~, namely $(H_i, H_p) = f^{-1}$(~~color).~~C). Since pond water is purely absorbing and ice is strongly scattering, the inverse function is well-defined., i.e. there exists a unique solution.

The incident solar spectrum covers the wavelength from 300 nm to 3000 nm (Grenfell and Perovich, 2008), but most of the long waves are absorbed in the first few ~~centimeters~~centimetres of water or ice because the absorption coefficients in the longwave band are larger than those in the shortwave band by at least two orders of magnitude (~~Fig. 4~~Warren, 1984). This means that the upwelling irradiance resulting from scattering in ice mainly consists of visible light. ~~In other words, the~~The color of melt ponds, which is produced by upwelling irradiance, is actually the response of the whole mass of pond water and its underlying ice regime to the incident solar spectrum, thus providing a theoretical possibility of retrieving the properties of pond water and its underlying ice from the apparent pond color.

On the other hand, the relationship between pond color and meltwater depth or sea-ice thickness has actually been qualitatively determined by many field investigations (e.g., Perovich et al., 2002a). Istomina et al. (2016) found that the underlying ice thickness has ~~an obvious~~a strong impact on the saturation value of pond color, but that the effect of pond depth is ~~negligible~~small. Variations in hue and luminance values of pond color are limited and ~~have nothing~~a relation to ~~do with~~ either H_i or H_p could not be observed. These results provided a quantitative validation of the relationship proposed here and also proved the possibility of ice property retrieval from pond color. The camera dependency of the relationship was highlighted and RAW format imagery was suggested to decrease this dependency.

Both RGB and HSL color spaces have been used in this study. Basically, they are just different mathematical descriptions of color, and there are no notable differences between them. The conversion between them is also simple. The HSL color space

is used to match the measurements by Istomina et al. (2016) and to examine the inverse problem $(H_i, H_p) = f^{-1}(H, S, L)$. A least-squares method is used, and the error function is defined as the Euclidean distance between the measured and simulated pond color ~~is defined as~~in the HSL color space:

~~$\Delta = |(H,S,L)_{\mathrm{SIM}} - (H,S,L)_{\mathrm{MEA}}|^2 = (H_{\mathrm{SIM}} - H_{\mathrm{MEA}})^2 + (S_{\mathrm{SIM}} - S_{\mathrm{MEA}})^2 + (L_{\mathrm{SIM}} - L_{\mathrm{MEA}})^2$,~~ ~~(7)~~

$$\Delta = |(H,S,L)_{\mathrm{SIM}} - (H,S,L)_{\mathrm{MEA}}| = \sqrt{c_H \cdot (H_{\mathrm{SIM}} - H_{\mathrm{MEA}})^2 + c_s \cdot (S_{\mathrm{SIM}} - S_{\mathrm{MEA}})^2 + c_L \cdot (L_{\mathrm{SIM}} - L_{\mathrm{MEA}})^2}\ , \quad (7)$$

where the subscript SIM denotes simulated results and MEA denotes *in-situ* measurements. The parameters c_H, c_S, and c_L indicate the different sensitivity of hue, saturation, and luminance values of pond color on pond depth and ice thickness, and they are determined by normalizing the square of correlation coefficient R^2 between the HSL values and the measured H_i and H_p. According to the statistical analyses in Istomina et al. (2016), there is c_H = 0.255, c_S = 0.712, and c_L = 0.033 (Table 1). Then an ergodic procedure using different combinations of H_i and H_p within reasonable ranges, 0–3 m for H_i and 0–0.5 m for H_p, can be performed to produce the minimum Δ, from which the ~~true~~estimated H_i and H_p can finally be determined. The retrievals of H_i and H_p using measured pond color by Istomina et al. (2016) and comparisons with field measurements are shown in Fig. ~~11~~10.

~~It is obvious from Fig. 11 that the point-to-point correlations between retrievals and measurements are less good than the results of melt-pond color in Fig. 10, implying that the inverse problem, $(H_i, H_p) = f^{-1}$(color), is more difficult to solve than the positive problem, (color) = $f(H_i, H_p)$. This is mainly attributed to the pond color, as the input of the inverse problem, which is more changeable than other parameters such as H_i, H_p and F_0 during field investigations. Besides, possible differences between in-situ conditions of sky and sea ice and the predefined values in this study can also partly explain the divergence.~~

A clear relationship between simulated and measured pond depth is not apparent in Fig. ~~11b~~10a, implying that the association of H_p with melt-pond color may be somewhat loose. This result agrees with Istomina et al. (2016). ~~In Fig. 11a, the~~The relationship between simulated and measured ice thickness is also not clear, but a good agreement can be found for thin ice with H_i < 1 m~~.~~ (Fig. 10b). This means, first, that the underlying ice thickness rather than the pond depth can be easily obtained from pond color, and second, that the present retrieval method is more suitable for thin ice than for thick ice.

The first statement can be partly explained by ~~Figs. 5c, 5d, and 5e~~Fig. 4, which ~~show~~shows that the dependence of pond color on ice thickness is obviously stronger than that on pond depth except for thick ice, H_i >1.5 m in Fig. ~~5c~~4c. Moreover, the upwelling irradiance comes mainly from scattering in ice, and therefore the pond color is associated more with the underlying ice than with the pond water. The second statement is ~~possibly~~ associated with the assumptions in the present RTM, which treats the pond water and underlying ice as parallel layers with uniform IOPs ~~(Fig. 2).~~ This assumption is ~~probably~~ more valid for thin FYI because FYI typically has larger, but shallower, ponds than MYI due to the rougher topography of MYI in general (Webster et al., 2015). Hence, measurements on MYI are more affected by the contrasts at the boundary between ponded and

带格式的: 字体: 倾斜

bare ice (Taskjelle et al., 2017), which depart from the definition of ~~Fig. 2~~the RTM. Another possible explanation comes from ice thickness since thin ice passes through more light than thick ice. With dark ocean beneath, the thinner domain shows a better discrimination as light at some wavelengths simply does not get backscattered, and that wavelength cutoff varies quickly with ice thickness.

Nevertheless, the result shown in Fig. ~~11~~10b is still encouraging. The squared correlation coefficient between simulated and measured ice thickness is $R^2 = 0.671$, and the correlation is significant ($P = 0.02$). The root-mean-square error is $\varepsilon = 0.156$ m. The relative error ξ, defined as the ratio of the absolute difference to the measured value, presents an average of 29% and a maximum of 50%. The result is acceptable because ~~it argues~~of the very few available data here. More validations from field observations are likely to improve the retrieve model in Eq. (7) and then reduce the error in retrievals.

The results give support for a possible new ~~way~~method of determining the sea-ice thickness, especially for melting sea ice~~, in contrast to the present situation where~~. This new method will complement our knowledge about sea ice thickness since presently most sea-ice thickness retrievals from satellite remote sensing are not good during the Arctic summer because of surface melt on ice (Kwok, 2010). ~~The accuracy of the H_i retrievals still has potential for improvement if more in-situ parameters such as F_0 and IOPs of ice can be concurrently obtained in future measurements.~~The limitations and applicability of the color-retrieval method are clear from the previous discussions. First, this method is valid for thin ice with thickness less than 1 m, and when the melt ponds on top of ice are open or just covered by very thin ice. Frozen melt ponds with a snow or thick ice cover, having an obviously different appearance from open ponds, are excluded from this method. Second, overcast sky conditions are preferable for this method. They are prevailing although not always present during summer in Arctic. However, further work is still needed to cover clear sky conditions. Finally, satellite remote sensing has been employed to determine MPF (e.g. Istomina et al., 2015), but it is still difficult for the satellite instruments to detect melt-pond color because of the small spatial scale of melt ponds. In contrast, hand-held photography (e.g. Istomina et al., 2016), ship-borne photography (e.g. Lu and Li, 2010), and airborne photography (e.g. Lu et al., 2010) are very effective ways to get the small-scale information on ice surface and provide a basis for ice thickness retrievals. Especially, with unmanned aerial vehicles (UAVs) equipped with a digital camera it is easy to observe sea ice surface features, including melt-pond color, at a floe scale, which has been successfully tested during the 7th Chinese Arctic cruise in 2016 (Wang et al., 2017).

5 Conclusions

A two-stream radiative transfer model was adopted and applied to ponded Arctic sea ice to examine the upwelling irradiance from the pond surface. A colorimetric method was provided to transform the upwelling spectrum into a color in the RGB color space, providing a way for comparisons with human vision and computer graphics. The dependence of pond color on the

带格式的: 缩进: 首行缩进: 0.5 字符

properties of the pond water and underlying sea ice was quantitatively and thoroughly investigated, and the use of pond color to retrieve the properties of ponded sea ice was also discussed.

The results reveal that both pond depth H_p and underlying ice thickness H_i have an important impact on pond color (Fig. ~~5~~4). The green and blue intensities increase only with increasing H_i except for very thick ice with $H_i > 4$ m, but the red intensity increases mostly with increasing H_i for thin ice ($H_i < 1.5$ m) and with increasing H_p for thick ice ($H_i > 1.5$ m), similarly to melt-pond albedo (LU16). The reproduced pond color gradually changes from dark blue to bright blue with increasing H_i, visually agreeing with in-situ photography of melt ponds in the Arctic summer.

The influence of the level of incident solar irradiance, F_0, is limited, but its spectral distribution can cause detectable variations in pond color. The incident solar spectrum has lower radiative energy in September than in August, but it is more concentrated at short wavelengths (< 530 nm) than at long wavelengths (> 530 nm) (Figs. ~~6~~5 and ~~7~~6). Then the red intensity decreases, whereas the blue intensity increases as F_0 changes from August to September.

The IOPs of meltwater and sea ice are prescribed in the present model. ~~However~~In nature, the optical properties of water are more stable than those of sea ice, which change with the microstructure of ice during melting (Light et al., 2004). A sensitivity study reveals that the influence of variations in sea-ice absorption coefficient is limited, but that scattering plays an important role in pond color (Fig. ~~8~~7). With increasing scattering in ice, all *rgb* intensities clearly increase, making the blue pond color brighter.

In a simplified melt case with $H_i + \delta H_p = 1.3$ m, where $\delta = 1.3$ the ratio of water and ice density, all *rgb* intensities of pond color decrease significantly from about 0.6 to 0.05, with the resulting color varying from gray to blue and then to black. The variation in red intensity is slightly different from those of green and blue: it is lower in value, and it drops linearly with ice melt, in contrast to the ~~superliner decline of the other two primary colors (Fig. 9).~~nonlinear decline of the other two primary colors (Fig. 8). In a real melt process, phase transition exists not only at ice surface but also in ice interior. If H_i and H_p are calculated by a thermodynamic model (e.g. Tsamados et al., 2015), and IOPs of sea ice are associated with ice physical parameters (e.g. Light et al., 2004), for example, ice porosity, then the seasonal evolutions in the color and albedo of melt ponds can be determined straightforwardly. However, it is out of the scope of the present paper and can be investigated in further studies.

The pond colors produced by the present model agree well with the pond-color measurements in the HSL color space reported by Istomina et al. (2016), proving the veracity of the proposed model and also implying the possibility of retrieving pond depth and ice thickness information from pond color~~.~~ (Fig. 9). A least-squares method was used to determine these quantities from three color components HSL. The results reveal a better agreement for ice thickness than for pond depth, and that the present

model provides better retrieval for thin FYI than for thick MYI ~~because~~. The former is attributed to be obviously higher dependence of pond color on ice thickness than on pond depth (Fig. 4). The latter is partly because that the plane-parallel assumption agrees more closely with ponds on flat sea ice than on rough ice, and also possibly due to the higher transparency of thin ice than thick ice.

As the first quantitative study on the color of melt ponds, this study investigated not only the extent to which pond color depends on various factors, such as H_i, H_p, F_0, and IOPs, but also illustrated a potential method to use pond-color data to obtain ice thickness. Many ways have been developed to obtain information on sea-ice thickness using remote-sensing technologies and drilling (Wadhams, 2005; Leppäranta, 2011), but none of them is easy and cheap to conduct in the Arctic, and most are not feasible under summer conditions. In comparison, retrieval of ice thickness from pond color has an obvious advantage over all other methods because ~~surface or aerial photography of melt ponds is easy to perform during field campaigns, and high-resolution optical satellite imagery can be used as well. Although the present retrieval algorithm is not highly robust, the~~hand-held, ship-borne or airborne photography of melt ponds, especially widespread UAVs equipped with a digital camera, is easy to perform during field campaigns, although the color-retrieval method is constrained by preconditions such as open melt ponds, thin ice, and overcast sky. A recent publication by Malinka et al. (2017) suggested another way to determine pond depth and ice thickness from measured spectral albedo of melt ponds. They obtained better retrievals of H_i and H_p partly because they used more complicated spectra as input compared with our case. As the first insight into the color of melt ponds, we tend to pose a possibility instead of draw a conclusion because of the limited available observations so far. The authors believe that more useful information can be extracted from the color of melt ponds if further in-situ validation data can be obtained and if the RTM can be improved to suit different ice types and sky conditions.

Acknowledgements. This research was supported by the Global Change Research Programme of China (2015CB953901), the National Natural Science Foundation of China (41676187 and 41376186). M.L. was supported by the EU FP7 Project EuRuCAS (European-Russian Centre for Cooperation in the Arctic and Sub-Arctic Environmental and Climate Research, Grant no. 295068) and the Academy of Finland (11409391), and B.C. was supported by the NSFC research facility mobility (41428603) and the Academy of Finland (283101). L.I. and G.H. conducted the study in the framework of the project: Spaceborne observations for detecting and forecasting sea ice cover extremes (SPICES) funded by the European Union (H2020) (Grant no. 640161). The authors are grateful to the scientific party of the ARK 27/3 cruise for making the sea ice optical measurements possible. Special thanks are expressed to Marcel Nicolaus for organizing the logistics and to the Sea Ice Physics group on board for assisting with the measurements. Three anonymous reviewers and the editor Jennifer Hutchings are also acknowledged for their constructive comments to highly improve the manuscript.

References

Adobe AGB (1998): Color image encoding. Availabe at www.Adobe.com, San Jose, USA, 2005.

Commission Internationale de l'Éclairage (CIE): Standard on colorimetric observers, CIE S002, 1986.

Eicken, H., Alexandrov, V., Gradinger, R., Ilyin, G., Ivanov, B., Luchetta, A., Martin, T., Olsson, K., Reimnitz, E., Pac, R., Poniz, P. and Weissenberger, J.: Distribution, structure and hydrography of surface melt puddles, Ber. Polarforsch, 149, 73–76, 1994.

Flocco, D., Feltham, D. L., Bailey, E. and Schroeder, D.: The refreezing of melt ponds on Arctic sea ice, J. Geophys. Res. Oceans, 120, 647–659, doi:10.1002/2014JC010140, 2015.

Flocco, D., Schroeder, D., Feltham, D. L. and Hunke, E. C.: Impact of melt ponds on Arctic sea ice simulations from 1990 to 2007, J. Geophys. Res., 117, C09032, doi:10.1029/2012JC008195, 2012.

Grenfell, T. C. and Perovich, D. K.: Radiation absorption coefficients of polycrystalline ice from 400–1400 nm, J. Geophys. Res., 86, 7447–7450, 1981.

Grenfell, T. C. and Perovich, D. K.: Incident spectral irradiance in the Arctic Basin during the summer and fall, J. Geophys. Res., 113, D12117, doi:10.1029/2007JD009418, 2008.

Guild, J.: The colorimetric properties of the spectrum, Phil. Trans. R. Soc. A, 230, 149–187, 1931.

Holland, M. M., Bailey, D. A., Briegleb, B. P., Light, B. and Hunke, E.C.: Improved sea ice shortwave radiation physics in CCSM4: the impact of melt ponds and aerosols on arctic sea ice, J. Clim., 25, 1413–1430, 2012.

Huang, W., Lei, R., Ilkka, M., Li, Q., Wang, Y. and Li, Z.: The physical structures of snow and sea ice in the Arctic section of 150 °–180 °W during the summer of 2010, Acta Oceanol. Sin., 32, 57–67, doi:10.1007/s13131-013-0314-4, 2013.

Huang, W., Lu, P., Lei, R., Xie, H. and Li, Z.: Melt pond distribution and geometry in high Arctic sea ice derived from aerial investigations, Ann. Glaciol., 57, doi:10.1017/aog.2016.30, 2016.

Hunke, E. C., Hebert, D. A. and Lecomte, O.: Level-ice melt ponds in the Los Alamos sea ice model, CICE, Ocean Model., 71, 26–42, 2013.

Hunt, R. G. W.: The reproduction of colour, 6th ed. John Wiley & Sons, pp. 844, 2004.

Istomina, L., Heygster, G., Huntemann, M., Marks, H., Melsheimer, C., Zege, E., Malinka, A., Prikhach, A. and Katsev, I.: Melt pond fraction and spectral sea ice albedo retrieval from MERIS data – Part 2: Case studies and trends of sea ice albedo and melt ponds in the Arctic for years 2002–2011, The Cryosphere, 9, 1567–1578, doi:10.5194/tc-9-1567-2015, 2015.

Istomina, L., Melsheimer, C., Huntemann, M., Nicolaus, M. and Heygster, G.: Retrieval of sea ice thickness during melt season from in situ, airborne and satellite imagery, IEEE International Geoscience and Remote Sensing Symposium (IGARSS), Beijing, 7678–7681, doi: 10.1109/IGARSS.2016.7731002, 2016.

Istomina, L., Nicolaus, M. and Perovich, D. K.: Spectral albedo of sea ice and melt ponds measured during POLARSTERN cruise ARK-XXVII/3 (IceArc) in 2012, Institut für Umweltphysik, Universität Bremen, doi:10.1594/PANGAEA.815111, 2013.

Istomina, L., Nicolaus, M. and Perovich, D. K.: Spectral albedo, water depth and ice thickness within melt ponds measured during POLARSTERN cruise ARK-XXVII/3 (IceArc) in 2012, Dataset #876210, DOI registration in progress, 2017.

Katlein, C., et al.: Influence of ice thickness and surface properties on light transmission through Arctic sea ice, J. Geophys. Res. Oceans, 120, doi:10.1002/2015JC010914, 2015.

Katlein, C., Nicolaus, M. and Petrich, C.: The anisotropic scattering coefficient of sea ice, J. Geophys. Res. Oceans, 119, doi:10.1002/2013JC009502, 2014.

Kilias, E. S., Peeken, I. and Metfies, K.: Insight into protist diversity in Arctic sea ice and melt-pond aggregate obtained by pyrosequencing, Polar Res., 33, 23466, doi:10.3402/polar.v33.23466, 2014.

Kwok, R.: Satellite remote sensing of sea-ice thickness and kinematics: a review, J. Glaciol., 56, 1129–1140, 2010.

Landy, J. C., Ehn, J. K. and Barber, D. G.: Albedo feedback enhanced by smoother Arctic sea ice, Geophys. Res. Lett., 42, doi:10.1002/2015GL066712, 2015.

Lang, A., Yang, S. and Kaas, E.: Sea ice thickness and recent Arctic warming, Geophys. Res. Lett., 44, 409–418, doi:10.1002/2016GL071274, 2017.

Leppäranta, M.: The drift of sea ice, 2nd ed. Springer-Praxis, Heidelberg, Germany, 2011.

Leppäranta, M., Reinart, A., Arst, H., Erm, A., Sipelgas, L. and Hussainov, M.: Investigation of ice and water properties and under-ice light fields in fresh and brackishwater bodies, Nord. Hydrol., 34, 245–266, 2003.

Light, B., Maykut, G. A. and Grenfell, T.C.: A temperature-dependent, structural-optical model of first-year sea ice, J. Geophys. Res., 109, C06013, doi:10.1029/2003JC002164, 2004.

Light, B., Perovich, D. K., Webster, M. A., Polashenski, C. and Dadic, R.: Optical properties of melting first-year Arctic sea ice, J. Geophys. Res. Oceans, 120, doi:10.1002/2015JC011163, 2015.

Lu, P., Leppäranta, M., Cheng, B. and Li, Z.: Influence of melt-pond depth and ice thickness on Arctic sea-ice albedo and light transmittance, Cold Reg. Sci. Technol., 124, 1–10, doi:10.1016/j.coldregions.2015.12.010, 2016.

Lu, P., and Li, Z.~~, Cheng, B., Lei, R. and Zhang, R.: Sea~~.: A method of obtaining ice ~~surface features in Arctic summer 2008: aerial observations,~~concentration and floe size from shipboard oblique sea ice images. IEEE T. Geosci. Remote Sens~~. Environ., 114(4): 693–699~~., 48(7), 2771-2780, 2010.

Lu, P., Li, Z., Cheng, B., Lei, R. and Zhang, R.: Sea ice surface features in Arctic summer 2008: aerial observations, Remote Sens. Environ., 114(4): 693–699, 2010.

Malinka, A., Zege, E., Istomina, L., Heygster, G., Spreen, G., Perovich, D., and Polashenski, C.: Reflective properties of melt ponds on sea ice, The Cryosphere Discuss., https://doi.org/10.5194/tc-2017-150, in review, 2017.

Nicolaus, M. and Katlein, C.: Mapping radiation transfer through sea ice using a remotely operated vehicle (ROV), The Cryosphere, 7, 763–777, doi:10.5194/tc-7-763-2013, 2013.

Nicolaus, M., Katlein, C., Maslanik, J. and Hendricks, S.: Changes in Arctic sea ice result in increasing light transmittance and absorption, Geophys. Res. Lett., 39, L24501, doi:10.1029/2012GL053738, 2012.

Perovich, D. K.: Theoretical estimates of light reflection and transmission by spatially complex and temporally varying sea ice covers, J. Geophys. Res. 95, 9557–9567, doi:10.1029/JC095iC06p09557, 1990.

Perovich, D. K.: The optical properties of sea-ice. Cold Reg. Res. and Eng. Lab. (CRREL) Report 96-1, 585 Hanover, NH, 1996

Perovich, D. K., Grenfell, T. C., Light, B. and Hobbs, P. V.: Seasonal evolution of the albedo of multiyear Arctic sea ice, J. Geophys. Res., 107, doi:10.1029/2000JC000438, 2002a.

Perovich, D. K., Tucker III, W. B. and Ligett, K. A.: Aerial observations of the evolution of ice surface conditions during summer, J. Geophys. Res., 107, doi:10.1029/2000JC000449, 2002b.

Perovich, D. K. and Polashenski, C.: Albedo evolution of seasonal Arctic sea ice, Geophys. Res. Lett., 39, L08501, doi:10.1029/2012GL051432, 2012.

Podgorny, I. A. and Grenfell, T. C.: Partitioning of solar energy in melt ponds from measurements of pond albedo and depth, J. Geophys. Res., 101(C10), 22737–22748, 1996.

Polashenski, C., Golden, K. M., Perovich, D. K., Skyllingstad, E., Arnsten, A., Stwertka, C. and Wright, N.: Percolation blockage: A process that enables melt pond formation on first year Arctic sea ice, J. Geophys. Res. Oceans, 122, doi:10.1002/2016JC011994, 2017.

Polashenski, C., Perovich, D. and Courville, Z.: The mechanisms of sea ice melt pond formation and evolution, J. Geophys. Res., 117, C01001, doi:10.1029/2011JC007231, 2012.

Rösel, A., Kaleschke, L. and Birnbaum, G.: Melt ponds on Arctic sea ice determined from MODIS satellite data using an artificial neural network, The Cryosphere, 6, 431–446, doi:10.5194/tc-6-431-2012, 2012.

Scott, F. and Feltham, D. L.: A model of the three-dimensional evolution of Arctic melt ponds on first-year and multiyear sea ice, J. Geophys. Res., 115, C12064, doi:10.1029/2010JC006156, 2010.

Smith, R. C. and Baker, K. S.: Optical properties of the clearest natural waters (200–800 nm), Appl. Optics, 20, 177–184, 1981.

Stiles, W. S. and Birch, J. M.: N.P.L. Colour-matching investigation: Final report (1958), Optica Acta., 6, 1–26, doi:10.1080/713826267, 1959.

Süsstrunk, S., Buckley, R. and Swen, S.: Standard RGB color spaces, Color and Imaging Conference, 7, 127–134, 1999.

Tanaka, Y., Tateyama, K., Kameda, T. and Hutchings, J. K.: Estimation of melt pond fraction over high concentration Arctic sea ice using AMSR-E passive microwave data, J. Geophys. Res. Oceans, 121, doi:10.1002/2016JC011876, 2016.

Taskjelle, T., Hudson, S. R., Granskog, M. A. and Hamre, B.: Modelling radiative transfer through ponded first-year Arctic sea ice with a plane parallel model, The Cryosphere Discuss., doi:10.5194/tc-2017-36, in review, 2017.

Tsamados, M., Feltham, D., Petty, A., Schroeder, D. and Flocco, D.: Processes controlling surface, bottom and lateral melt of Arctic sea ice in a state of the art sea ice model, Phil. Trans. R. Soc. A, 373, 20140167, doi:/10.1098/rsta.2014.0167, 2015.

Wadhams, P.: Arctic sea ice thickness-A review of current technique and future possibilities, Proceedings of International Workshop on Arctic Sea Ice Thickness: past, present, and future, Denmark, 12–23, 2005.

Warren, S. G.: Optical constants of ice from the ultraviolet to the microwave, Appl. Optics, 23, 1206-1225, 1984.

Wang, M., Su, J., Li, T., Wang, X., Ji, Q., Cao, Y., Lin, L., Liu, Y.: Study on the method of extracting Arctic melt pond and roughness information on sea ice surface based on UAV observation, Chinese J. Polar Res., 29(4), 436–445, 2017. (In Chinese)

Webster, M. A., Rigor, I. G., Perovich, D. K., Richter-Menge, J. A., Polashenski, C. M. and Light, B.: Seasonal evolution of melt ponds on Arctic sea ice, J. Geophys. Res. Oceans, 120, doi:10.1002/2015JC011030, 2015.

Wright, W. D.: A re-determination of the trichromatic coefficients of the spectral colours, Trans. Opt. Soc., 30, 141–164, 1928.

Zege, E., Malinka, A., Katsev, I., Prikhach, A., Heygster, G., Istomina, L., Birnbaum, G. and Schwarz, P.: Algorithm to retrieve the melt pond fraction and the spectral albedo of Arctic summer ice from satellite optical data, Remote Sens. Environ., 163, 153–164, 2015.

Table 1: The squared correlation coefficients R^2 between melt-pond color and H_I and H_P in Istomina et al. (2016), and the deduced coefficients c_H, c_S, and c_L for Eq. (7).

Parameter	Coefficient	R^2		
		Total	H_I	H_P
Hue	0.255 (c_H)	0.301	0.266	0.035
Saturation	0.712 (c_S)	0.842	0.759	0.083
Luminosity	0.033 (c_L)	0.039	0.020	0.019

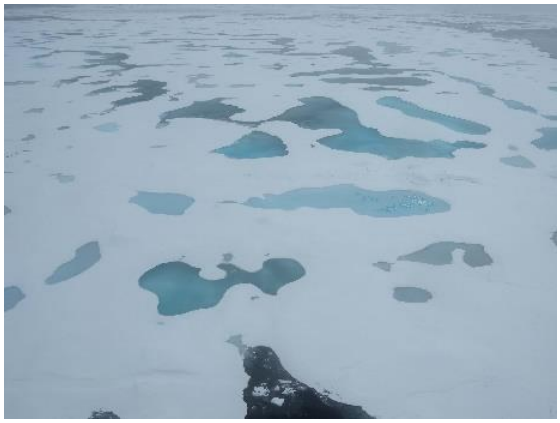

Figure 1: A typical image of melt ponds on Arctic sea ice captured onboard R/V *Xuelong* during the Chinese National Arctic Research Expeditions in summer 2016, clearly illustrating the large variability of pond color even on the same ice floe.

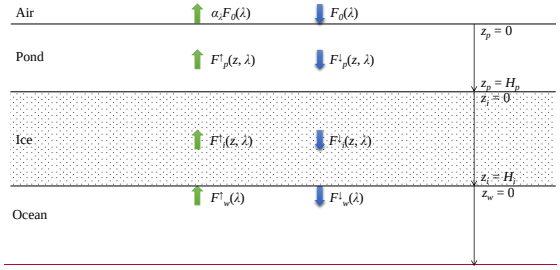

~~**Figure 2: Schematic graph of the radiative transfer model for melt ponds on Arctic sea ice in LU16. $F_0(\lambda)$ is the incident solar irradiance. $F^{\uparrow}(z, \lambda)$ and $F^{\downarrow}(z, \lambda)$ are the upwelling and downwelling irradiances, and z is the depth, with subscripts p, i, w for the layer of pond water, the underlying ice, and the ocean respectively. H_p is the pond depth, H_i is the thickness of the underlying ice, α_s is the spectral melt-pond albedo, and λ is the wavelength, which is constrained within the visible band in this study.**~~

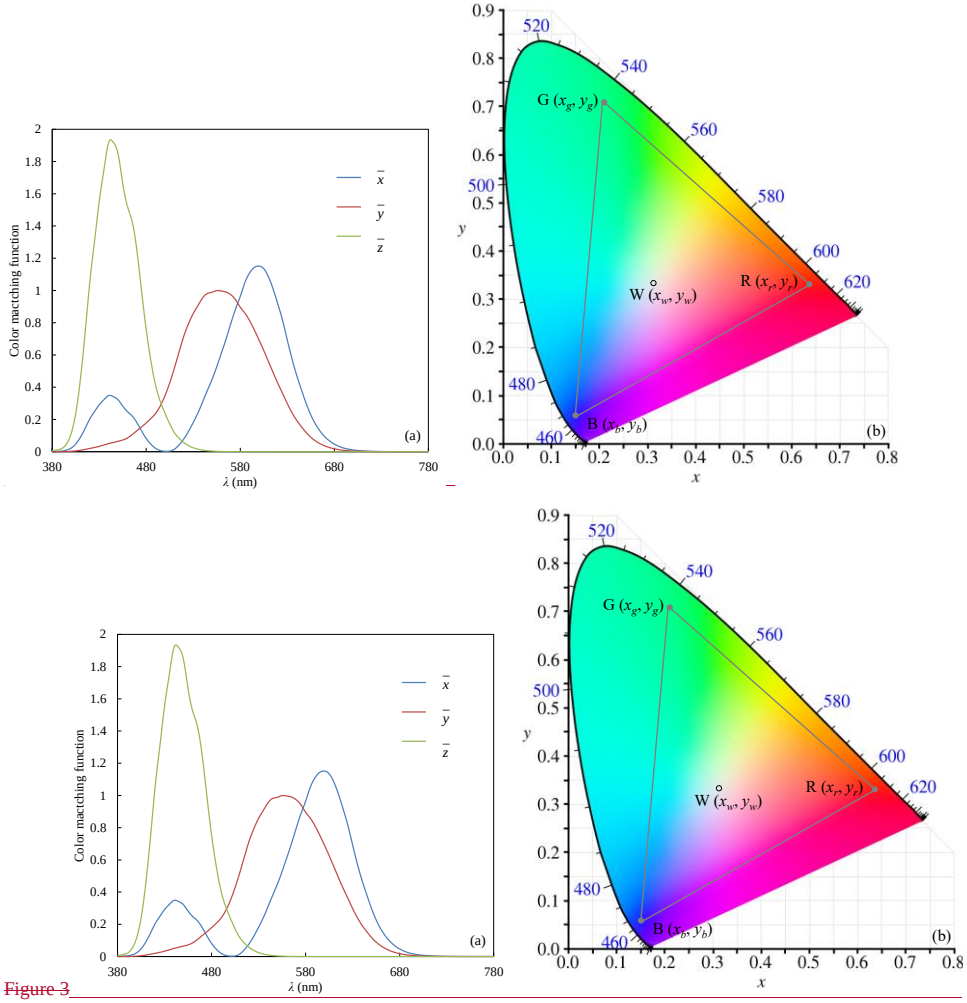

~~Figure 3~~

Figure 2: (a) The CIE color matching functions $\bar{x}(\lambda)$, $\bar{y}(\lambda)$, and $\bar{z}(\lambda)$, and (b) the CIE color space chromaticity diagram. The outer curved boundary is the spectral (or monochromatic) locus, with wavelengths shown in nanometers. R, G, and B are the primary colors of red, green and blue, and W is the position of the white color.

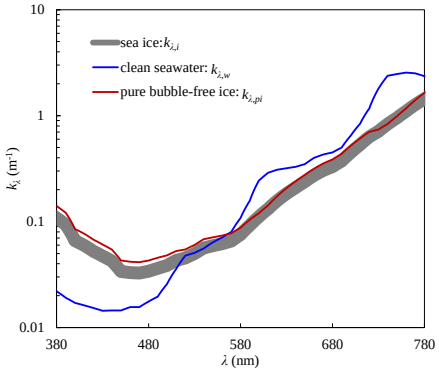

Figure 43: Absorption coefficients of clean seawater, pure bubble-free ice and sea ice in the visible band ~~according to LU16.~~. The water data are from Smith and Baker (1981). The pure ice data are from Grenfell and Perovich (1981) and Warren (1984). The $k_{\lambda,i}$ value was calculated from $k_{\lambda,i} = v_{pi}k_{\lambda,pi} + v_{bp}k_{\lambda,w}$, based on the volume fractions $v_{pi} \geq 60\%$ and $v_{bp} \leq 20\%$ ($v_{pi} + v_{bp} \leq 100\%$) from field observations of summer Arctic sea ice (Huang et al., 2013).

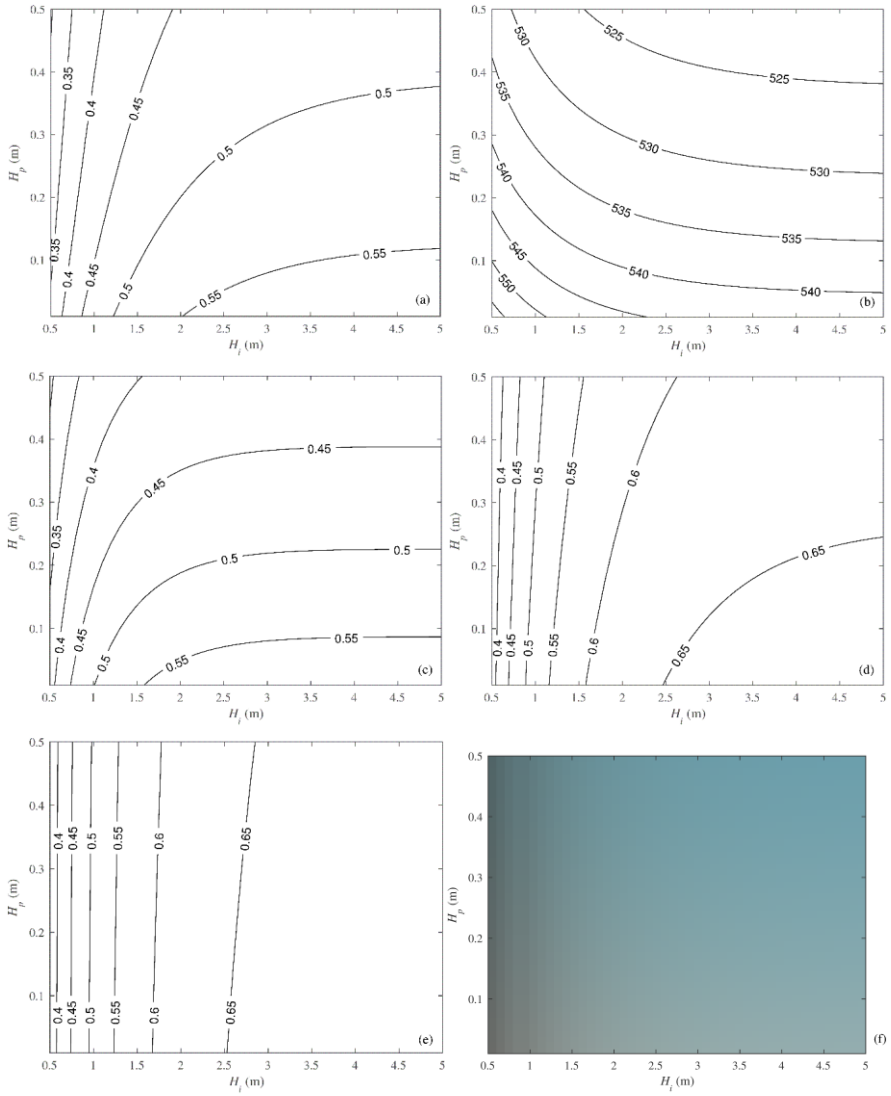
(a)
(b)
(c)
(d)
(e)
(f)
H_p (m)
H_i (m)

Figure ~~5~~4: Variations of melt-pond optics and color with pond depth and underlying ice thickness: (a) integrated pond albedo α_B, (b) mean wavelength determined by Eq. (~~3~~1), (c–e) intensities of red, green, and blue components scaled in the range of 0–1, (f) ~~true~~simulated color of the melt pond in the RBG color space~~.~~ according to the colorimetric method defined by Eqs. (2-6). The sky condition is ~~completely~~ overcast.

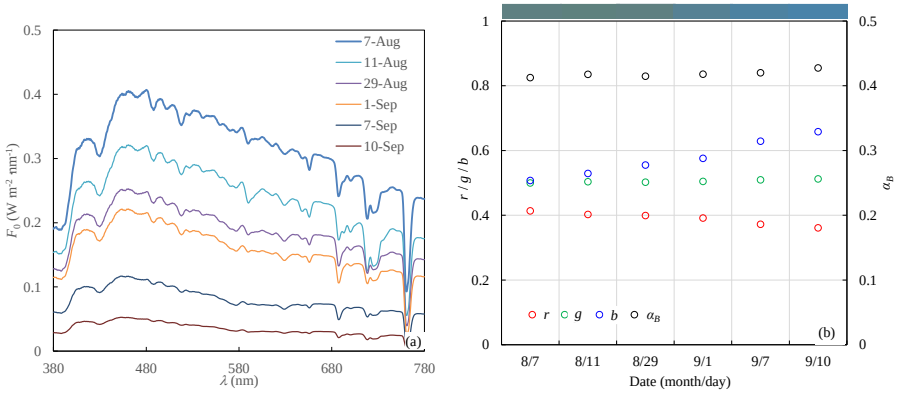

Figure ~~6~~5: (a) Typical spectral incident solar irradiances in the Arctic summer under a completely overcast sky according to Grenfell and Perovich (2008), and (b) their influence on melt-pond albedo and the *rgb* intensities of pond color for H_p = 0.3 m and H_i = 1.0 m. The color bar on top of (b) denotes the ~~true~~simulated color of the melt pond under different sky conditions.

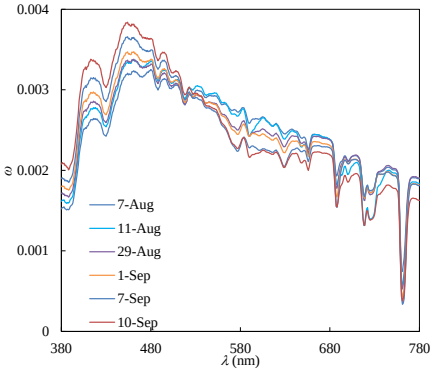

Figure ~~7~~6: Normalized values of incident solar radiation under different sky conditions, defined as the ratio of the spectrum in Fig. ~~6a~~5a to the total energy in the visible band.

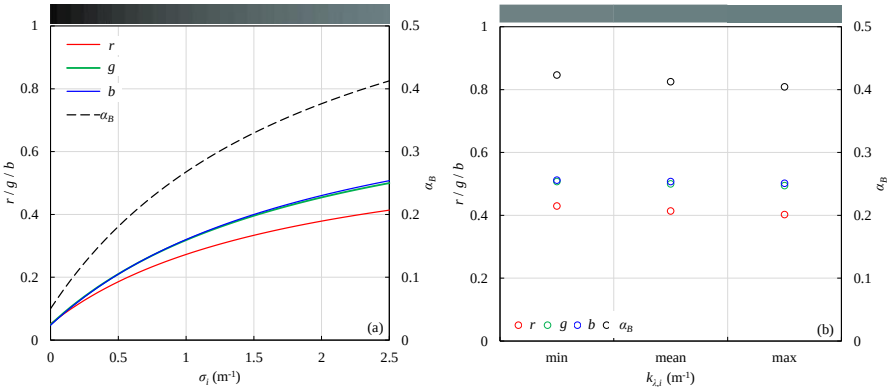

Figure ~~87~~: Variation of the *rgb* intensities of pond color and melt-pond albedo with the inherent optical properties of underlying sea ice: (a) scattering coefficient and (b) absorption coefficient for H_p = 0.3 m and H_i = 1.0 m. The color bar on top denotes the ~~true~~simulated color of the melt pond under different optical properties of sea ice.

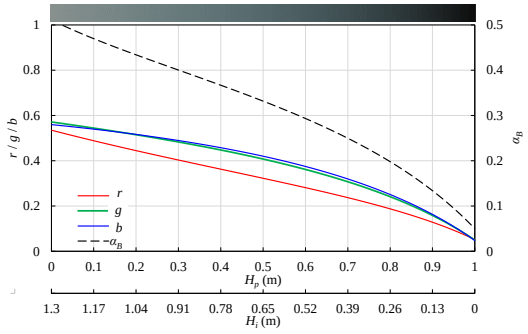

Figure ~~98~~: Variations of the *rgb* intensities of pond color and melt-pond albedo during the process of sea-ice melting, assuming H_i + δH_p = 1.3 m. The color bar on the top denotes the ~~true~~simulated color of the melt pond during ice melting.

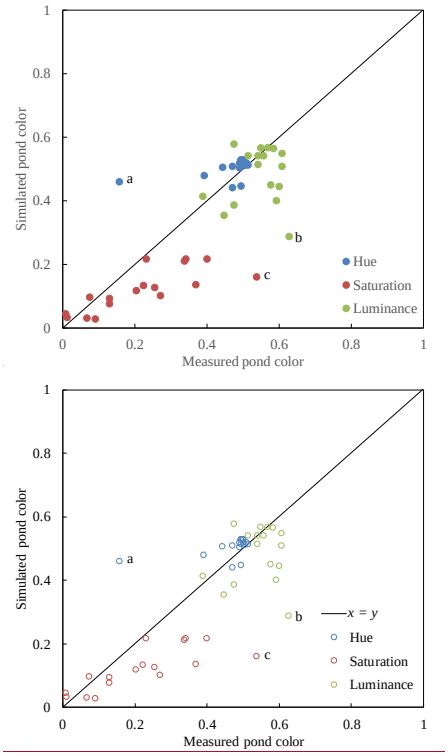

Figure ~~10~~9: Comparisons of simulated pond color with in-situ measurements by Istomina et al. (2016) in the HSL color space. ~~The solid line is the boundary *x = y*.~~ Points a, b, and c are special cases discussed in the text.

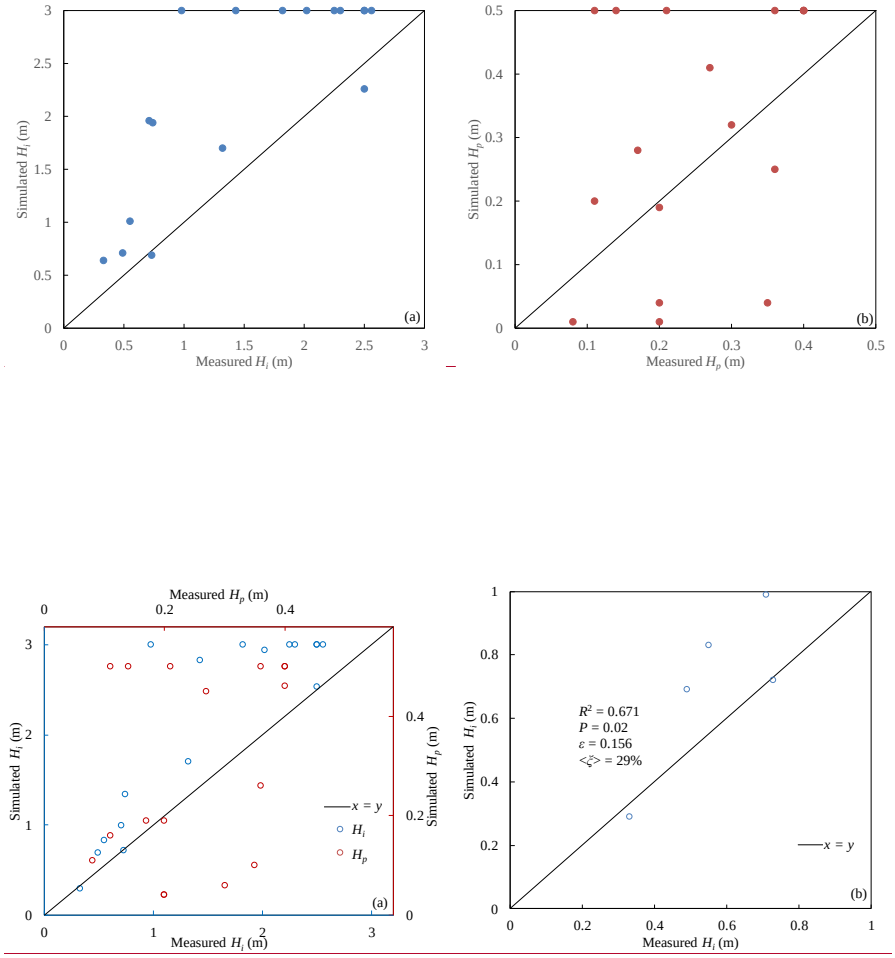

Figure ~~11:~~10: (a) Retrievals of ~~(a)~~ underlying ice thickness and ~~(b)~~ pond depth using measured pond colors in Istomina et al. (2016). (b) is a subset of (a) for H_i < 1 m. R is the correlation coefficient between simulated and measured H_i. P is the significance level of the correlation. ε is the root-mean-square error, and <ξ> is the mean of relative error in simulated H_i.